



Published in final edited form as:

Neurobiol Dis. 2018 September ; 117: 125–136. doi:10.1016/j.nbd.2018.05.021.

Pretangle pathology within cholinergic nucleus basalis neurons coincides with neurotrophic and neurotransmitter receptor gene dysregulation during the progression of Alzheimer's disease

Chelsea T. Tiernan^a, Stephen D. Ginsberg^{b,c,d,e}, Bin He^f, Sarah M. Ward^a, Angela L. Guillozet-Bongaarts^g, Nicholas M. Kanaan^{a,h}, Elliott J. Mufson^f, and Scott E. Counts^{a,h,i,j,*}

^aDepartment of Translational Science and Molecular Medicine, Michigan State University, Grand Rapids, MI, USA

^bCenter for Dementia Research, Nathan Kline Institute, Orangeburg, NY, USA

^cDepartment of Psychiatry, NYU Langone School of Medicine, New York, NY, USA

^dDepartment of Physiology & Neuroscience, NYU Langone School of Medicine, New York, NY, USA

^eNYU Neuroscience Institute, NYU Langone School of Medicine, New York, NY, USA

^fDepartment of Neurobiology, Barrow Neurological Institute, Phoenix, AZ, USA

^gAllen Institute for Brain Science, Seattle, WA, USA

^hHauenstein Neurosciences Center, Mercy Health Saint Mary's Hospital, Grand Rapids, MI, USA

ⁱDepartment of Family Medicine, Michigan State University, Grand Rapids, MI, USA

^jMichigan Alzheimer's Disease Core Center, Ann Arbor, MI, USA

Abstract

Cholinergic basal forebrain neurons of the nucleus basalis of Meynert (nbM) regulate attentional and memory function and are exquisitely prone to tau pathology and neurofibrillary tangle (NFT) formation during the progression of Alzheimer's disease (AD). nbM neurons require the neurotrophin nerve growth factor (NGF), its cognate receptor TrkA, and the pan-neurotrophin receptor p75^{NTR} for their maintenance and survival. Additionally, nbM neuronal activity and cholinergic tone are regulated by the expression of nicotinic (nAChR) and muscarinic (mAChR) acetylcholine receptors as well as receptors modulating glutamatergic and catecholaminergic afferent signaling. To date, the molecular and cellular relationships between the evolution of tau pathology and nbM neuronal survival remain unknown. To address this knowledge gap, we profiled cholinergic pathway genes within nbM neurons immunostained for pS422, a pretangle phosphorylation event preceding tau C-terminal truncation at D421, or dual-labeled for pS422 and TauC3, a later stage tau neo-epitope revealed by this same C-terminal truncation event, via single-

*Corresponding author at: Department of Translational Science and Molecular Medicine, Department of Family Medicine, Michigan State University, College of Human Medicine, 400 Monroe Ave NW, Grand Rapids, MI 49503, USA. scott.counts@hc.msu.edu (S.E. Counts).

Declaration of conflicts of interest

None of the authors has any conflicts of interest related to this study or its reported findings.

population custom microarray analysis. nbM neurons were obtained from postmortem tissues from subjects who died with an antemortem clinical diagnosis of no cognitive impairment (NCI), mild cognitive impairment (MCI), or mild/moderate AD. Quantitative analysis revealed significant downregulation of mRNAs encoding TrkA as well as TrkB, TrkC, and the Trk-mediated downstream pro-survival kinase Akt in pS422+ compared to unlabeled, pS422-negative nbM neurons. In addition, pS422+ neurons displayed a downregulation of transcripts encoding NMDA receptor subunit 2B, metabotropic glutamate receptor 2, D2 dopamine receptor, and β 1 adrenoceptor. By contrast, transcripts encoding p75^{NTR} were downregulated in dual-labeled pS422+/TauC3+ neurons. Appearance of the TauC3 epitope was also associated with an upregulation of the α 7 nAChR subunit and differential downregulation of the β 2 nAChR subunit. Notably, we found that gene expression patterns for each cell phenotype did not differ with clinical diagnosis. However, linear regression revealed that global cognition and Braak stage were predictors of select transcript changes within both unlabeled and pS422+/TauC3TM neurons. Taken together, these cell phenotype-specific gene expression profiling data suggest that dysregulation of neurotrophic and neurotransmitter signaling is an early pathogenic mechanism associated with NFT formation in vulnerable nbM neurons and cognitive decline in AD, which may be amenable to therapeutic intervention early in the disease process.

Keywords

Cholinergic basal forebrain; Mild cognitive impairment; Nucleus basalis of Meynert; Trk receptor; Neurotrophin; Acetylcholine receptor; Glutamate receptor; Dopamine receptor; Adrenoceptor; Neurotransmission

1. Introduction

Cholinergic projection neurons originating within the region of the substantia innominata termed the nucleus basalis of Meynert (nbM) provide the major source of acetylcholine to the cortical mantle (Mesulam et al., 1983). Cholinergic nbM neurons regulate memory and attention (Baxter and Chiba, 1999) and undergo progressive degeneration in Alzheimer's disease (AD) that correlates with disease progression and degree of cognitive impairment (Bierer et al., 1995). Recent work from our group suggests that the cascade of pathophysiological events leading to cholinergic nbM neuronal degeneration in AD is associated with the appearance of discrete epitopes within the microtubule-associated protein tau (Tiernan et al., 2016b), which are progressively revealed as this protein undergoes a pathological sequence of post-translational modifications precipitating the formation of neurofibrillary tangles (NFTs) in AD (Braak et al., 1994; García-Sierra et al., 2003; Ghoshal et al., 2002; Ghoshal et al., 2001; Guillozet-Bongaarts et al., 2005).

Cholinergic tone of nbM neurons is regulated by the expression of receptors for acetylcholine (AChRs) and other neurotransmitters, as well as receptors for nerve growth factor (NGF) and related neurotrophins. Cholinergic neurotransmission is mediated pre- and post-synaptically by nicotinic acetylcholine receptors (nAChRs) through ligand-gated cation influx (Gotti et al., 1997), and muscarinic acetylcholine receptors (mAChRs) through G-protein-coupled receptor-mediated pathways (Levey, 1996). nbM neurons receive

cholinergic afferents (Smiley and Mesulam, 1999) and express both nAChRs (Breese et al., 1997) and mAChRs (Mufson et al., 1998). In addition, immunohistochemical evidence exists for the regulation of cholinergic signaling through several afferent systems, including glutamatergic, dopaminergic, and noradrenergic projections as well as local GA-BAergic interneurons (Smiley and Mesulam, 1999).

The viability of cholinergic nbM neurons is dependent upon the binding, internalization, and retrograde transport of NGF, which is mediated by the cognate NGF receptor tyrosine kinase TrkA and the pan-neurotrophin receptor p75^{NTR} (Counts and Mufson, 2005; Kaplan and Miller, 2000; Mufson et al., 2003; Sofroniew et al., 2001). Other neurotrophin receptor tyrosine kinase family members including TrkB, which preferentially binds brain-derived neurotrophic factor (BDNF), and TrkC, which binds neurotrophin-3 (NT-3), are also localized to nbM neurons, albeit at lower levels of expression than TrkA, suggesting that neurotrophic signaling through these receptors also contribute to nbM functionality (Ginsberg et al., 2006; Mufson et al., 2002a; Salehi et al., 1996).

Perturbation in the expression of both AChRs and neurotrophin receptors are observed in nbM neurons during the clinical progression of AD. Specifically, we reported that gene expression of *Chrna7* (encoding the $\alpha 7$ nAChR subunit) is upregulated in nbM neurons isolated postmortem from mild/moderate AD subjects compared to subjects who died with mild cognitive impairment (MCI) or no cognitive impairment (NCI) (Counts et al., 2007). Additionally, transcripts encoding the cognate NGF, BDNF, and NT-3 receptors TrkA, TrkB, and TrkC, respectively, are downregulated in cholinergic neurons in MCI and AD subjects as compared to NCI subjects and correlate with cognitive decline and neuropathology (Ginsberg et al., 2006), consistent with reports of loss of TrkA immunoreactivity in the nbM during prodromal and frank disease (Mufson et al., 2000). In contrast, we observed that *Ngfr* transcripts (encoding p75^{NTR}) remain steady throughout clinical disease progression (Ginsberg et al., 2006); however, a phenotypic silencing of p75^{NTR} immunoreactivity is observed in nbM neurons of MCI and AD subjects (Mufson et al., 2002b). While the expression patterns of these AChR and neurotrophin receptor mRNAs appears to follow clinical disease progression, recent work from our group suggests that specific stages of tau pathology and not clinical disease status drive differential gene regulation in nbM neurons (Tiernan et al., 2016b).

In the present study, we evaluated the extent to which levels of transcripts encoding neurotrophin receptors, AChRs, and additional neurotransmitter receptors change with the pathological evolution of NFTs in vulnerable nbM neurons. Expression profile mosaics were quantified in individual nbM neurons immunostained for the pS422 tau epitope, a “pretangle” phosphorylation event at the S422 residue that occurs early in the pathological evolution of NFTs, or TauC3, a later stage tau neopeptide revealed by caspase-mediated cleavage at D421 (Gamblin et al., 2003; Guillozet-Bongaarts et al., 2005, 2006; Vana et al., 2011). Phenotypically distinct neurons were microdissected from tissue sections obtained postmortem from subjects who died with an antemortem clinical diagnosis of NCI, MCI, or AD, followed by gene expression analysis using custom-designed microarrays. Our data demonstrate that dysregulation of select genes regulating the expression of nAChR subunits and neurotrophin receptors, as well as select downstream signaling molecules, are

differentially associated with appearance of the pS422 and TauC3 epitopes, lending further support to the hypothesis that early pathological events underlying nbM cholinotropic abnormalities and neuronal vulnerability are related to the progression of tau pathology. Furthermore, select transcripts regulating glutamatergic, GABAergic, dopaminergic, serotonergic, and noradrenergic signaling were also altered along with tau pathological stage, suggesting a shift in afferent firing patterns within the nbM that would in turn affect cholinergic tone in nbM projection zones.

2. Materials and methods

2.1. Subjects

Demographic, clinical, and neuropathological characteristics of the subjects are summarized in Table 1. Custom-designed microarray analysis of single nbM neurons was performed using tissue obtained postmortem from 28 participants in the Rush Religious Orders Study (RROS) (Bennett et al., 2002; Counts et al., 2014; Ginsberg et al., 1997; Mufson et al., 1999) who were clinically diagnosed within a year of death with NCI (n = 10), MCI (n = 10), or mild/moderate AD (n = 8). Details of clinical evaluations and diagnostic criteria in the RROS cohort have been extensively published (Bennett et al., 2002; Counts et al., 2006; Ginsberg et al., 2006; Mufson et al., 1999; Perez et al., 2015a). Briefly, a team of investigators performed an annual clinical examination, including neuropsychological performance testing using the Mini-Mental State Exam (MMSE) and 17 additional neuropsychological tests referable to episodic memory, semantic memory, working memory, perceptual speed, and visuospatial ability. A Global Cognitive Score (GCS), consisting of a composite z-score calculated from this test battery, was determined for each participant (Bennett et al., 2002; Counts et al., 2006; Ginsberg et al., 2006; Mufson et al., 1999; Perez et al., 2015a). A board-certified neurologist with expertise in the evaluation of the elderly made the clinical diagnosis based on impairments in each of the five cognitive domains and a clinical examination. The diagnosis of dementia or AD met recommendations by the joint working group of the National Institute of Neurologic and Communicative Disorders and Stroke/AD and Related Disorders Association (NINCDS/ADRDA) (Chen et al., 1984). The MCI population was defined as subjects who exhibited cognitive impairment on neuropsychological testing but did not meet the clinical criteria for AD or dementia, which is consistent with the diagnostic criteria used by others in the field (Petersen et al., 2001).

Tissue samples were obtained and processed as previously published (Counts et al., 2006; Mufson et al., 1999; Tiernan et al., 2016b). At autopsy, the cerebrum was slabbed into 1 cm sections and one hemisphere was immersion-fixed in 4% paraformaldehyde in 0.1 M phosphate buffer, pH 7.2 for 24–72 h at 4 °C followed by cryoprotection; the opposite hemisphere was snap frozen. Paraffin-embedded fixed tissue sections from select regions (e.g., hippocampus and neocortex) were examined for amyloid and neuritic plaque pathology, NFTs, Lewy bodies, and TDP-43 inclusions (Bennett et al., 2002; Mufson et al., 2016). A board-certified neuropathologist blinded to the clinical diagnosis performed the neuropathological evaluation and classified individual cases based on the NIA–Reagan, Consortium to Establish a Registry for Alzheimer’s Disease (CERAD), and Braak staging

criteria (Braak and Braak, 1991; Hyman et al., 2012; Mirra et al., 1991; Mufson et al., 2016).

2.2. Double-label immunohistochemistry for microarray analysis

Fixed tissue blocks containing the substantia innominata were sectioned at 40 μm on a freezing-sliding microtome in 1:18 series and cryoprotected. Immunohistochemistry to identify pS422- and TauC3-immunopositive neurons in the anteromedial nbM subfields has been detailed previously (Tiernan et al., 2016b). Briefly, the presence of intact RNA was confirmed in each case by acridine orange histofluorescence (Ginsberg et al., 1997). The peroxidase-quenching, blocking, avidin-biotin complex labeling, and all rinsing steps were performed as previously described (Tiernan et al., 2016b). The primary antibodies used were TauC3 (1:5000), a mouse monoclonal IgG1 raised against D421-cleaved tau (Gamblin et al., 2003), and pS422 (1:15,000; Invitrogen, 44-764G), a polyclonal rabbit IgG antibody directed against the phospho-tau epitope pS422. In addition, adjacent nbM sections in each case were immunostained with p75^{NTR} to demonstrate the presence of cholinergic magnocellular neurons, as previously described (Mufson et al., 1989; Tiernan et al., 2016b). Primary antibodies were incubated with tissue overnight at 4 °C, followed by a 2 h incubation with biotinylated goat anti-mouse IgG [heavy plus light (H + L) chains] secondary antibody (1:500; BA-9200) for TauC3, or biotinylated goat anti-rabbit IgG (H + L) (1:500; BA-1000) for pS422 (both from Vector Labs). Labeling was developed with Vector SG peroxidase substrate (SK-4700) to yield a dark blue reaction product in TauC3-immunopositive (TauC3+) neurons, and 0.05% 3,3'-diaminobenzidine (DAB; Sigma, D5637) containing 0.03% hydrogen peroxide to yield a reddish-brown reaction product in pS422-immunolabeled (pS422+) profiles. Tissue sections were slide mounted, and processed for Nissl counterstaining using Cresyl violet (Kanaan et al., 2010) to identify immunonegative nbM neurons and to aid in cytoarchitectonic analysis, and stored at 4 °C without cover-slipping prior to microdissection.

2.3. Double-labeled immunofluorescence for confocal microscopy

Confocal microscopy was performed to confirm the presence of three discretely labeled neuronal populations as previously described (Tiernan et al., 2016b). Tissue was blocked, incubated with primary antibodies overnight (pS422, 1:2500; TauC3, 1:10,000), labeled with secondary antibodies (pS422 with Alexa Fluor 488 goat anti-rabbit; TauC3 with Alexa Fluor 594 goat anti-mouse; Invitrogen, A-11008 and A-11005), and washed with DAPI (1:10,000; Invitrogen, D1306) to counterstain cell nuclei. Following the staining procedure, sections were mounted on microscope slides, autofluorescence was blocked using Sudan black as described (Kanaan et al., 2007; Tiernan et al., 2016b), and coverslipped using hardset Vectashield mounting media.

2.4. Single cell microaspiration, TC RNA amplification, and array hybridization

nbM neurons displaying one of four phenotypes were microdissected: 1) Nissl-positive but immunonegative (unlabeled), 2) single labeled pS422+, 3) dual-labeled pS422/TauC3-immunopositive (pS422+/TauC3+), and 4) single labeled TauC3+ nbM neurons were accessed using either a micromanipulator and micro-controlled vacuum source (Eppendorf, Westbury, NY) attached to a Nikon TE2000 inverted microscope (Fryer, Huntley, IL)

(Bennett et al., 2002; Counts et al., 2014; Ginsberg et al., 2010b; Mufson et al., 2002a) or an Arcturus XT laser capture microdissection (LCM) instrument (ThermoFisher, South San Francisco, CA). Approximately 50–60 neurons per phenotype were individually analyzed by the custom-designed microarrays (Ginsberg, 2005; Ginsberg et al., 2006, 2010a).

RNA amplification from nbM neurons was performed using terminal continuation (TC) RNA amplification methodology (Alldred et al., 2009; Che and Ginsberg, 2004; Ginsberg, 2005), as previously described (Counts et al., 2014; Tiernan et al., 2016b). Briefly, microaspirated nbM neurons were homogenized in 500 μ l Trizol reagent (ThermoFisher, Waltham, MA). RNAs were reverse transcribed in the presence of the poly d(T) primer (100 ng/ μ l) and TC primer (100 ng/ μ l) in 1 \times first strand buffer (ThermoFisher), 2 μ g of linear acrylamide (ThermoFisher, Foster City, CA), 10 mM dNTPs, 100 μ M DTT, 20 U of SuperRNase Inhibitor (Life Technologies), and 200 U of reverse transcriptase (Superscript III, ThermoFisher). Single-stranded cDNAs were digested with RNase H and re-annealed with the primers in a thermal cycler: RNase H digestion step at 37 $^{\circ}$ C, 30 min; denaturation step 95 $^{\circ}$ C, 3 min; primer re-annealing step 60 $^{\circ}$ C, 5 min. This step generated cDNAs with double-stranded regions at the primer interface. Samples were then purified by column filtration (Montage PCR filters; EMD Millipore, Billerica, MA). Hybridization probes were synthesized by in vitro transcription using 33 P-UTP incorporation in 40 mM Tris (pH 7.5), 6 mM MgCl₂, 10 mM NaCl, 2 mM spermidine, 10 mM DTT, 2.5 mM ATP, GTP and CTP, 100 μ M of cold UTP, 20 U of SuperRNase Inhibitor, 2 KU of T7 RNA polymerase (Epicentre Illumina, Madison, WI), and 120 μ Ci of 33 P-UTP (Perkin-Elmer, Boston, MA) (Alldred et al., 2009; Counts et al., 2014; Ginsberg et al., 2010a; Petersen et al., 2001). The reaction was performed at 37 $^{\circ}$ C for 4 h. Radiolabeled TC RNA probes were hybridized to custom-designed microarrays without further purification. Arrays were hybridized overnight at 42 $^{\circ}$ C in a rotisserie oven and washed sequentially in 2 \times SSC/0.1% SDS, 1 \times SSC/0.1% SDS, and 0.5 \times SSC/0.1% SDS for 20 min each at 42 $^{\circ}$ C. Arrays were placed in a phosphor screen for 24 h and developed on a Storm phosphor imager (GE Healthcare, Piscataway, NJ).

2.5. Custom-designed microarray platforms and data collection

Array platforms consisted of 1 μ g linearized cDNA purified from plasmid preparations adhered to high-density nitrocellulose (Hybond WL, GE Healthcare). Approximately 576 cDNAs of interest to neurobiology and neurodegeneration were utilized on the array platform (Ginsberg et al., 2017; Tiernan et al., 2016b). Hybridization signal intensity was determined using Image Quant software (GE Healthcare) and quantified by subtracting background using an empty vector (pBluescript). Expression of TC amplified RNA bound to each linearized cDNA minus background was expressed as a ratio of the total hybridization signal intensity of the array (i.e., global normalization) (Counts et al., 2014, 2006; Ginsberg, 2005; Mufson et al., 1999; Perez et al., 2015b). The data analysis generated expression profiles of relative changes in mRNA levels among the phenotypically distinct nbM neurons dissected from each case within the clinical diagnostic groups. Each neuron was analyzed in triplicate via three independent probe amplifications and array hybridizations using the original neuronal cDNA pool as template.

2.6. Data analysis and statistics

Demographic variables (Table 1) were compared among clinical diagnostic groups by Kruskal-Wallis or Fisher's Exact tests with Bonferroni correction for pairwise comparisons. Relative changes in total hybridization signal intensity of individual mRNAs were analyzed by one-way ANOVA with post-hoc Newman-Keuls analysis for multiple comparisons. The level of statistical significance was set at $p < 0.05$. A false discovery rate controlling procedure was used to reduce type I errors due to the large number of genes analyzed simultaneously (Allred et al., 2015; Che and Ginsberg, 2004; Counts et al., 2007; Hyman et al., 2012; Mirra et al., 1991; Reiner et al., 2003). Expression levels of select mRNAs were clustered and displayed using a bioinformatics and graphics software package (GeneLinker Gold, Improved Outcomes, Kingston, ON). The relationship between select transcript level changes and independent demographic and clinical pathologic variables within unlabeled, pS422+, and pS422+/TauC3+ nbM neurons was assessed by linear regression.

3. Results

3.1. Subject demographics

Clinical and neuropathological characteristics of the 28 cases (10 NCI, 10 MCI, and 8 mild/moderate AD) included in the microarray analysis are summarized in Table 1. No significant differences were observed for age, gender balance, years of education, or postmortem interval. The ApoE4 allele was more frequent in AD compared to NCI, but the MCI cohort was not significantly different from either NCI or AD. The AD group performed significantly poorer on the MMSE compared to the NCI and MCI groups ($p < 0.0001$), whereas GCS z-scores declined progressively throughout the transition from NCI to MCI to AD ($p < 0.0001$). Distribution of Braak scores was significantly different across the clinical groups. The NCI cases displayed significantly lower Braak scores than MCI or AD ($p = 0.004$). NCI cases were classified as Braak stages I/II (40%) or III/IV (60%). No NCI cases were Braak stage V-VI. The MCI cohort met the criteria for Braak stages I/II (20%), III/IV (50%), and V/VI (30%), and AD subjects were classified as Braak stages I/II (12.5%), III/IV (25%), and V/VI (62.5%). NIA-Reagan diagnosis significantly differentiated NCI cases from MCI and AD subjects ($p = 0.002$), and CERAD scores were significantly higher in AD compared to NCI and MCI ($p = 0.01$).

3.2. nbM neuronal tau phenotypes

nbM tau pathology was marked by double-label immunohistochemical staining for the pretangle phospho-epitope pS422 and the mature NFT neopeptide TauC3 (Vana et al., 2011). pS422+ staining exhibited a reddish-brown reaction product that filled the neuronal cytoplasm and labeled many neurites (Fig. 1A, B). TauC3+ staining produced a dark blue reaction product that discretely filled the cytoplasm of neurons that were often shrunken or misshapen (Fig. 1A, B). Confocal analysis confirmed the presence of three discrete populations of nbM neurons expressing early, intermediate, or late stage NFT pathology (Fig. 1C–F). For gene expression analysis, individual unlabeled, pS422+, pS422+/TauC3+, or TauC3+ nbM neurons were microdissected.

3.3. nbM neurotrophin receptor-related gene expression

Expression profiling was performed on approximately 250 custom-designed microarrays following TC RNA amplification. Combining single neuron expression profiling with tau site-specific antibodies allowed for the characterization of the temporal molecular events associated with NFT formation within nbM neurons during the progression of AD. Quantitative analyses compared the signal intensities of transcripts either between clinical disease stages or between tau neuronal phenotypes. Comparison of transcript levels in pS422+ nbM neurons microaspirated from each clinical group revealed no statistical differences (Fig. 2). However, when analyzed independent of clinical diagnosis, expression levels of key transcripts regulating neurotrophin receptor expression and function were altered by the phenotypic transition from unlabeled to pS422+ to pS422+/TauC3+ to TauC3+ in nbM neurons (Fig. 3).

Compared to unlabeled neurons, nbM neurons bearing the pretangle phospho-epitope pS422 revealed a significant downregulation of six mRNAs encoding the intracellular tyrosine kinase (TK) and extracellular (ECD) domains of the neurotrophin receptors TrkA (*Ntrk1* TK, 50%, $p < 0.001$; *Ntrk1* ECD, 53%, $p < 0.001$), TrkB (*Ntrk2* TK, 45%, $p < 0.001$; *Ntrk2* ECD, 42%, $p < 0.001$), and TrkC (*Ntrk3* TK, 38%, $p < 0.01$; *Ntrk3* ECD, 35%, $p < 0.01$), as well as two mRNAs encoding signaling molecules downstream of neurotrophin receptor activity, the serine/threonine-specific protein kinases protein kinase B (*Akt1*, 50%, $p < 0.01$) and protein kinase C (PKC)- ϵ (*Prkce*, 50%, $p < 0.01$). Interestingly, expression levels of the mRNA encoding the pan-neurotrophin receptor p75^{NTR} (*Ngfr*) did not decrease until appearance of the TauC3 epitope (40% decrease, $p < 0.01$). Cleavage at D421 was also associated with the upregulation of one downstream signaling molecule, PKC- α (*Prkca*, 36% increase, $p < 0.01$). Loss of the pS422 phenotype in mature NFTs (e.g., TauC3+ only) was not associated with any additional mRNA expression changes.

3.4. Tau pathology and nbM cholinergic neuronal marker-related gene expression

There were no significant differences in the relative expression levels of any genes regulating acetylcholine synthesis, release, or degradation in nbM neurons throughout the progression from prefibrillar to mature NFT tau pathology (Fig. 4), including choline acetyltransferase (*Chat*), vesicular acetylcholine transporter (*Slc18a3*), acetylcholinesterase (*Ache*), and butyrylcholinesterase (*Bche*). Similarly, expression of the muscarinic acetylcholine receptors M1 (*Chrm1*) and M2 (*Chrm2*) remained comparable across pathological states of tau. By contrast, mRNA expression of two nicotinic acetylcholine receptor subunits, $\alpha 7$ (*Chrna7*) and $\beta 2$ (*Chrb2*), were differentially regulated following appearance of the TauC3 epitope. *Chrna7* was significantly upregulated (50% increase, $p < 0.01$), whereas *Chrb2* was significantly downregulated (40% decrease, $p < 0.05$).

3.5. Tau pathology and neurotransmitter gene expression in nbM neurons

With respect to glutamate receptors, nbM neurons bearing the pS422 pretangle epitope revealed a significant downregulation of ionotropic NMDA receptor subunit 2B (*Grin2B*, 50% $p = 0.001$) and metabotropic glutamate receptor 2 (*Grm2*, 55%, $p < 0.001$) compared to unlabeled neurons (Fig. 5), whereas select transcripts encoding NMDA receptor subunit 1 (*Grin1*), AMPA receptor subunits 1 (*Gria1*) and 2 (*Gria2*), and kainate receptor subunits 1

(*Grik1*) and 4 (*Grik4*) were significantly downregulated with the appearance of the TauC3 epitope (Table 2). Catecholamine receptors were also dysregulated with pretangle pathology, as 50–60% decreases in D2 dopamine receptor (*Drd2*, $p < 0.001$) and $\beta 1$ adrenoceptor (*Adra1b*, $p < 0.001$) transcript levels were observed in pS422+ neurons (Fig. 5). The appearance of the TauC3 epitope within nbM neurons coincided with a downregulation of additional dopaminergic (*Drd1*, 40%, $p = 0.02$; *Drd4*, 45%, $p = 0.008$) and noradrenergic (*Adra2a*, 45%, $p = 0.003$; *Adra2b*, 50%, $p = 0.005$) receptor gene expression.

3.6. Microarray validation

qPCR and immunoblot validation analyses of frozen tissue samples were not conducted as previously described (Allred et al., 2015; Ginsberg et al., 2010b, 2010a, 2006), since any changes associated with these phenotypes at the single neuron level would likely be masked by regional gene expression patterns from admixed neuronal and non-neuronal cell types (Ginsberg et al., 2012). On the other hand, the upregulation of neuronal *Chrna7* during AD has been reported by both in situ hybridization and immunohistochemical approaches (Counts et al., 2007; Hellström-Lindahl et al., 1999; Teaktong et al., 2004). Future studies employing single population RNA-sequencing, Fluidigm, and/or Nanostring nCounter analyses are warranted when single population transcriptomic technologies become more standardized and economical (Buettner et al., 2015; Kim et al., 2015; Macosko et al., 2015) for human postmortem tissue use.

3.7. Relationships among expression level, demographics, and clinical pathologic variables for select transcripts

Although alterations in transcript levels were related to the progressive appearance of pretangle and NFT tau epitopes as compared to clinical diagnosis, we tested whether transcript levels within each nbM neuronal phenotype were associated with age, postmortem interval, GCS, MMSE scores, Braak stage, CERAD diagnosis, and/or Reagan diagnosis using multivariate linear regression. Neither age nor postmortem interval was a predictor for expression level changes of any of the transcripts analyzed (not shown). By contrast, both GCS and Braak stage predicted transcript levels for *Nrtk1* TK, *Nrtk2* TK, and *Grin2b* in unlabeled nbM neurons, whereas GCS alone predicted transcript level changes for *Adrab1* (Table 3). In pS422+ nbM neurons, GCS, MMSE score, and Braak stage predicted *Nrtk1* TK, *Nrtk2* TK, and *Grin2b* transcript levels, whereas GCS was also a predictor for *Nrtk3* TK, *Grm2*, *Drd2*, and *Adrab1* (Table 3). Reagan diagnosis was also predicted to influence levels of *Nrtk1* and *Adrab1* transcripts in pS422+ neurons. None of the independent variables predicted expression levels for the transcripts in pS422+/TauC3+ nbM neurons. Notably, *Ngfr*, *Chrna7* and *Chrb2* levels were not associated with clinical pathologic variables (not shown).

4. Discussion

The present study reveals that dysregulation of mRNAs encoding select neurotrophin and neurotransmitter receptors critical for nbM function and cortical cholinergic tone coincides with progressive intraneuronal post-translational modifications of tau that lead to NFT formation. In addition, alterations in several of these mRNAs (e.g., *Nrtk1*, *Nrtk2*, *Grii2B*,

Adrab1) were associated clinical pathologic variables - particularly GCS and Braak stage - in unlabeled and pS422+ nbM neurons, suggesting a correlation among neurotrophic and neurotransmitter abnormalities, worsening global cognition, and the global spread of neurofibrillary pathology as tau pretangles accumulate within cholinergic nbM projection neurons.

Cholinergic nbM neurons rely on NGF and its cognate (TrkA) and pan-neurotrophin (p75^{NTR}) receptors for proper cellular function and survival (Counts and Mufson, 2005; Lad et al., 2003). Many previous reports have identified an early deficit in nbM neurotrophic support, namely a phenotypic downregulation of TrkA expression in MCI and early AD (Chu et al., 2001; Counts et al., 2004; Mufson et al., 2000). Here, we demonstrate that downregulation of transcripts encoding TrkA and its family members TrkB and TrkC, within individual nbM neurons coincides with the pre-tangle tau pathological marker pS422, suggesting that cholinergic nbM neuronal survival is compromised prior to the formation of mature NFTs. We cannot ascertain causality at this point, and whether pathological changes in tau drive diminished TrkA expression in nbM neurons is unclear. However, TrkA expression is under positive feedback from NGF (Holtzman et al., 1992; Li et al., 1995), and this pathway may be disrupted during the progression of dementia by reduced retrograde transport of cortical NGF to nbM consumer neurons (Mufson et al., 1995; Scott et al., 1995). While aggregated wild-type tau is a known inhibitor of anterograde fast axonal transport (Kanaan et al., 2012, 2011; LaPointe et al., 2009), there is some evidence to suggest that phosphorylation at S422 impairs retrograde transport, as well (Tiernan et al., 2016a). Thus, phosphorylation of tau at S422 and the resulting inhibition of retrograde transport may impair positive feedback from NGF leading to a loss of TrkA expression on the nbM neuronal cell surface. It is also possible that diminished TrkA expression does not result from pathological maturation of tau and/or impaired retrograde transport of NGF, but rather some other mechanism related to the binding and internalization of NGF at the terminal or activation of downstream signal transduction pathways (Klesse and Parada, 1999; Sofroniew et al., 2001). Future analysis of the potential interactions between aberrant tau phosphorylation and disrupted neurotrophic signaling in cholinergic nbM neurons is warranted in cohorts such as the RROS as well as in relevant animal and cellular models.

TrkA maintains nbM neuronal viability through a number of signal transduction pathways, including MAPK/CREB, PI3K, and PLC γ (Kaplan and Miller, 2000; Klesse and Parada, 1999; Lad et al., 2003; Sofroniew et al., 2001). The present findings suggest that appearance of the pS422 epitope in nbM neurons is associated with alterations in some but not all of these signal transduction pathways. Appearance of the pS422 epitope was not associated with expression level changes in *Mapk1*, *Mapk3*, or *Creb1*, suggesting that transcriptional regulation of the MAPK/CREB pathway in nbM neurons is unaffected by pathogenic modification of tau. Conversely, expression of genes encoding the serine/threonine kinase Akt (*Akt1*) and the calcium-modulated PKC- ϵ isozyme (*Prkce*) were downregulated in pS422-positive nbM neurons, whereas PKC- α (*Prkca*) was upregulated with the appearance of TauC3. Akt is the principal downstream mediator of PI3K (Burgering and Coffey, 1995; Datta et al., 1996; Franke et al., 1997; Klippel et al., 1996), promoting cell survival through a phosphorylation cascade that prevents the insertion of pro-apoptotic Bax proteins into the mitochondrial membrane (Dudek et al., 1997; Gross et al., 1998; Putcha et al., 1999). PKC-

α and PKC- ϵ are components of the PLC γ pathway, which promotes survival following activation by PLC γ -mediated hydrolysis of PI 4,5-P2 to diacylglycerol (Bell and Burns, 1991; Nishizuka, 1988; Sofroniew et al., 2001). The dysregulation of these three kinases suggests that two of the principal signal transduction pathways mediating nbM neuronal survival, PI3K and PLC γ , may be compromised during the formation of mature NFTs.

Ngfr transcripts encoding p75^{NTR} were not significantly reduced until appearance of the TauC3 epitope, suggesting that this receptor is functional during the early stages of tau pathology but is down-regulated in nbM neurons progressing into the later stages of NFT formation. p75^{NTR} bifunctionally mediates a signal to induce or inhibit cell death, depending on a variety of factors including the co-expression of Trk receptor family members and the presence of pro- or mature forms of neurotrophins (Carter et al., 1996; Casaccia-Bonofil et al., 1996; Hempstead et al., 1991; Mamidipudi and Wooten, 2002; Miller and Kaplan, 2001; Roux and Barker, 2002). When expressed together, p75^{NTR} positively regulates signaling through TrkA by enhancing the specificity and binding of NGF (Barker and Shooter, 1994; Berg et al., 1991; Hempstead et al., 1991; Mahadeo et al., 1994), which in turn promote cell survival. In the absence of TrkA, p75^{NTR} has been demonstrated to mediate both anti-apoptotic and pro-apoptotic effects. For example, in the presence of NGF, p75^{NTR} can rescue peripheral cell cultures from apoptosis (Gentry et al., 2000; Roux et al., 2001). However, in central neurons and oligodendrocytes, NGF stimulation of p75^{NTR} in the absence of TrkA more commonly triggers apoptosis (Casaccia-Bonofil et al., 1996; Frade et al., 1996; Friedman, 2000; Yoon et al., 1998). A putative proapoptotic role for p75^{NTR} has been demonstrated following the withdrawal of neurotrophic support (Martin et al., 1988). Mechanisms underlying NGF withdrawal-mediated apoptosis likely involves activation of the JNK pathway and consequent release of cytochrome *c* and caspase activation (Bruckner et al., 2001; Eilers et al., 2001; Harding et al., 2001; Martinou et al., 1999; Putcha et al., 1999), as well as activation of the cell cycle regulating molecules cyclin-dependent kinases 4/5 (Park et al., 1997, 2000, 1998). Interestingly, we have previously reported an increase in *Casp3*, *Casp7*, and *Cdk5* in TauC3-immunopositive nbM neurons (Tiernan et al., 2016b), suggesting that p75^{NTR}-dependent apoptosis may be actively occurring in cells expressing the mature NFT marker, TauC3. An additional mechanism of p75^{NTR}-mediated cell death may involve accumulation of the NGF precursor protein proNGF. While cortical levels of mature NGF remain steady during the progression of AD (Mufson et al., 2003), proNGF levels increase by 40–60% in the cortex of subjects diagnosed with MCI or mild AD compared with NCI (Peng et al., 2004). TrkA protein levels were found to be reduced in the cortex in early stage AD compared to p75^{NTR} levels (Counts et al., 2004), and both reduced TrkA levels and increased proNGF levels in the cortex were associated with poorer antemortem cognitive performance (Counts et al., 2004; Peng et al., 2004). Our present finding that TrkA expression is relatively downregulated in pS422+ nbM neurons compared to p75^{NTR}, taken together with the accumulation of pS422+ nbM neurons in MCI and AD (Vana et al., 2011), suggests a pathologic link between pretangle pathology and a shift from pro-survival to pro-apoptotic signaling in nbM neurons (Counts and Mufson, 2005; Masoudi et al., 2009; Mufson et al., 2007). This process is likely exacerbated upon appearance of TauC3+ NFT pathology, when p75^{NTR} expression is reduced.

Appearance of the TauC3 neoepitope was also associated with the differential regulation of two nAChR subunits, upregulation of $\alpha 7$ and downregulation of $\beta 2$. $\alpha 7$ subunits are likely expressed as homodimeric assemblies, whereas $\beta 2$ co-assembles with $\alpha 4$ as a heterodimer. Together, $\alpha 7$ homodimer and $\alpha 4\beta 2$ heterodimer nAChRs constitute the two major nAChR subtypes expressed in the brain (Gotti et al., 1997). Upregulation of $\alpha 7$ nAChR mRNA has been demonstrated previously in subjects diagnosed with mild/moderate AD compared to NCI and MCI, however no change in the $\beta 2$ nAChR subunit was reported (Counts et al., 2007). This discrepancy likely results from the more stringent phenotypic selection of nbM neurons based on tau pathology that was used in the present investigation. There is some evidence from PET imaging studies to suggest that the $\alpha 4\beta 2$ nAChR subtype is down-regulated in MCI and AD (Kendziorra et al., 2010; Terrière et al., 2010), however ours is the first report to suggest interplay between expression of the $\alpha 7$ homodimer and $\alpha 4\beta 2$ heterodimer during the progression of AD. Overall, the present results suggest that appearance of the TauC3 epitope may shift the cell surface stoichiometry of neuronal nAChRs from heterodimeric $\alpha 4\beta 2$ to homodimeric $\alpha 7$ subtypes.

Pretangle pathology in nbM neurons was associated with decreased expression of select glutamatergic, dopaminergic, and noradrenergic receptors. Downregulation of *Drd2* and *Adra1b* may be related to dysfunction and neurodegeneration of catecholaminergic systems, including the ventral tegmental area and locus coeruleus (Bondareff et al., 1987; Gibb et al., 1989; Mann et al., 1980), during the progression of AD, which would cause dysregulation of inputs to the cholinergic nbM (Jones and Cuello, 1989; Smiley and Mesulam, 1999; Smiley et al., 1999; Zaborszky and Cullinan, 1996). In particular, we and others have shown that locus coeruleus noradrenergic neuron loss occurs very early in the disease process (Arendt et al., 1985, 2015; Kelly et al., 2017; Theofilas et al., 2017) and likely contributes to disruptions in cholinergic modulation of attentional function. Glutamate-mediated excitotoxicity has been implicated in AD neuronal dysfunction and cognitive impairment, and dysregulation of the *Grin2B*-encoded NMDA receptor 2B subunit appears to be a primary pathogenic event in disease progression (Andreoli et al., 2013; Hu et al., 2012; Olney et al., 1997). GRIN2B plays a crucial role in learning and memory (Cao et al., 2007; Tang et al., 2001), and its expression is reduced in the entorhinal cortex and hippocampus of the AD brain (Bi and Sze, 2002; Sze et al., 2001). The present results extend these findings to the nbM, and suggest that perturbations in NMDA receptor activation and functionality may induce excitotoxic neuronal injury (Farber et al., 1998), which manifests as cognitive impairment. A role for excitotoxicity-mediated neuronal injury in nbM neurons is also suggested by the presently observed decrease in the *Gria2*-encoded AMPA 2 receptor subunit following appearance of the TauC3 epitope. The AMPA 2 subunit significantly influences calcium permeability of AMPA receptor gated ion channels, whereby its coexpression with other AMPA receptor subunits produces channels with little to no calcium permeability (Hollmann et al., 1991). Loss of *Gria2* expression would result in increased intracellular calcium levels through unopposed activation of the calcium permeable subunits GRIA4/5, which were unaltered presently. Hence, these findings reinforce the potential contribution of calcium dysregulation to tangle formation in nbM neurons (Ahmadian et al., 2015; Riascos et al., 2014; Wu et al., 2005) and implicate glutamate-mediated excitotoxicity as a potential mediator of this pathogenic process.

5. Conclusions

These results derived from single-population analysis of nbM neurons with defined tau pathology status suggest that neurotrophic receptor expression and functionality in cholinergic nbM neurons is compromised prior to the onset of frank NFT pathology, and early impairments of neurotrophic and neurotransmitter signaling play a substantial role in nbM cholinergic tone and survival. We and others have previously reported some of these cholinotropic changes in individual nbM neurons during the progression from NCI to MCI to AD (Chu et al., 2001; Counts et al., 2007, 2004; Mufson et al., 2002a, 2000, 1997; Salehi et al., 1996); however, here we demonstrate in a well-characterized clinical pathological cohort that these alterations are associated with specific stages of tau pathology, supporting the hypothesis that the accumulation of pathological tau epitopes in nbM neurons drives neurodegenerative processes that contribute to the clinical progression of AD (Mesulam et al., 2004; Tiernan et al., 2016b; Vana et al., 2011). Limitations of this study include the fact that this postmortem human tissue-based study is inherently correlative and cannot address causality, underscoring the need for more detailed mechanistic experimentation in relevant preclinical models to understand the sequence of events that link tau pathology to potential deleterious alterations in neuronal gene expression regulation. In summary, dysregulation of neurotrophic cell survival and afferent glutamatergic and catecholaminergic signaling is an early pathogenic mechanism associated with NFT formation in vulnerable cholinergic nbM neurons in AD, which provide new clues for translational approaches to therapeutic intervention.

Acknowledgements

We thank John Beck and Muhammad Nadeem for excellent technical assistance. We are indebted to the altruism of the RROS participants.

Funding

This work was supported by NIH grants AG014449 (CTT, SDG, NMK, EJM, SEC), AG053581 (SEC), AG053760 (SEC), NS082730 (NKM), AG044372 (NKM), AG043375 (EJM, SDG), AG107617 (SDG), AG19610 (EJM) as well as the Alzheimer's Association grant IIRG-11-203928 (SDG), Thorek Memorial Foundation (SEC, NKM), Saint Mary's Foundation (SEC), Miles for Memories of Battle Creek, MI (SEC), and the Barrow Neurological Institute Barrow and Beyond (EJM).

Abbreviations:

Ache

acetylcholinesterase

AD

Alzheimer's disease

Adra2a, Adra2b, Adra1b

adrenoceptor alpha 2a, alpha 2b, beta 1

Akt1

Akt serine/threonine protein kinase 1/protein kinase B

ApoE
apolipoprotein E

Bche
butyrylcholinesterase

BDNF
brain derived neurotrophic factor

Casp3,7
caspases 3,7

Cdk5
cyclin-dependent kinase 5

CERAD
Consortium to Establish a Registry for Alzheimer's Disease

Chat
choline acetyltransferase

Creb1
cAMP regulatory element binding protein

Drd1–5
dopamine receptor D1–D5

ECD
extracellular domain

Gabbr1
gamma-aminobutyric acid (GABA) type B receptor subunit 1

Gabra1–6
GABA type A receptor subunit alpha 1–6 subunit

Gabrb1–3
GABA type A receptor subunit beta 1–3 subunit

Gabrd
GABA type A receptor subunit delta

Galr1–3
galanin receptor 1–3

GCS
Global Cognitive Score

Gria1–4
AMPA receptor subunit 1–4

Grik1–5

kainite receptor subunit 1–5

Grin1, Grin2a-d

NMDA receptor subunits 1, 2A–D

Grm1–8

metabotropic glutamate receptor 1–8

Htr1b

5-hydroxytryptamine (serotonin) receptor 1B

Htr2b,c

serotonin receptor 2B, C

Htr3,7

serotonin receptor 3, 7

JNK

c-jun N-terminal kinase

mAChR (Chrm1,2)

cholinergic receptor, muscarinic 1, 2

MAPK, Mapk1, 3

mitogen-activated protein kinase 1 (Erk2), 3 (Erk1)

MCI

mild cognitive impairment

MMSE

Mini-Mental State Exam

nAChR (Chrna7, Chrna4, Chrn2)

cholinergic receptor, nicotinic, alpha polypeptide 7, alpha polypeptide 4, beta polypeptide 2

nbM

nucleus basalis of Meynert

NCI

no cognitive impairment

NFT

neurofibrillary tangle

NGF

nerve growth factor

NT-3

neurotrophin-3

PI3K

phosphatidylinositol 3 kinase

Prkca, Prkce, Prkci

protein kinase C (PKC) alpha, epsilon, iota

PLC γ , phospholipase C- γ ; pS422

phosphorylation of tau at serine-422

p75^{NTR} (*Ngfr*)

nerve growth factor receptor

RROS

Rush Religious Order Study

Slc18a3

vesicular acetylcholine transporter

TauC3

antibody directed against tau truncated at aspartic acid-421

TC

terminal continuation

TK

intracellular tyrosine kinase domain

TrkA (*Ntrk1*), TrkB (*Ntrk2*), TrkC (*Ntrk3*)

neurotrophin tyrosine kinase receptor type 1, 2, 3

References

- Ahmadian SS, Rezvanian A, Peterson M, Weintraub S, Bigio EH, Mesulam M-M, Geula C, 2015 Loss of calbindin-D28K is associated with the full range of tangle pathology within basal forebrain cholinergic neurons in Alzheimer's disease. *Neurobiol. Aging* 36, 3163–3170. <http://dx.doi.org/10.1016/j.neurobiolaging.2015.09.001>. [PubMed: 26417681]
- Allred MJ, Che S, Ginsberg SD, 2009 Terminal continuation (TC) RNA amplification without second strand synthesis. 177, 381–385. <http://dx.doi.org/10.1016/j.jneumeth.2008.10.027>.
- Allred MJ, Lee SH, Petkova E, Ginsberg SD, 2015 Expression profile analysis of vulnerable CA1 pyramidal neurons in young-middle-aged Ts65Dn mice. *J. Comp. Neurol.* 523, 61–74. <http://dx.doi.org/10.1002/cne.23663>. [PubMed: 25131634]
- Andreoli V, De Marco EV, Trecroci F, Cittadella R, Di Palma G, Gambardella A, 2013 Potential involvement of GRIN2B encoding the NMDA receptor subunit NR2B in the spectrum of Alzheimer's disease. *J. Neural Transm.* 7, 574 <http://dx.doi.org/10.1074/jbc.M700050200>.
- Arendt T, Bigl V, Tennstedt A, Arendt A, 1985 Neuronal loss in different parts of the nucleus basalis is related to neuritic plaque formation in cortical target areas in Alzheimer's disease. *Neuroscience* 14, 1–14. [PubMed: 3974875]

- Arendt T, Bruckner MK, Morawski M, Jager C, Gertz H-J, 2015 Early neurone loss in Alzheimer's disease: cortical or subcortical? *Acta Neuropathol. Commun.* 3, 10 <http://dx.doi.org/10.1186/s40478-015-0187-1>. [PubMed: 25853173]
- Barker PA, Shooter EM, 1994 Disruption of NGF binding to the low affinity neurotrophin receptor p75 LNTR reduces NGF binding to TrkA on PC12 cells. *Neuron* 13, 203–215. [PubMed: 7519025]
- Baxter MG, Chiba AA, 1999 Cognitive functions of the basal forebrain. *Curr. Opin. Neurobiol.* 9, 178–183. [PubMed: 10322180]
- Bell RM, Burns DJ, 1991 Lipid activation of protein-kinase-C. *J. Biol. Chem.* 266, 4661–4664. [PubMed: 2002013]
- Bennett DA, Wilson RS, Schneider JA, Evans DA, Beckett LA, Aggarwal NT, Barnes LL, Fox JH, Bach J, 2002 Natural history of mild cognitive impairment in older persons. 59, 198–205.
- Berg MM, Sternberg DW, Hempstead BL, Chao MV, 1991 The low-affinity p75 nerve growth factor (NGF) receptor mediates NGF-induced tyrosine phosphorylation. *PNAS* 88, 7106–7110. [PubMed: 1714587]
- Bi H, Sze CI, 2002 N-methyl-D-aspartate receptor subunit NR2A and NR2B messenger RNA levels are altered in the hippocampus and entorhinal cortex in Alzheimer's disease. *J. Neurol. Sci.* 200, 11–18. [PubMed: 12127670]
- Bierer LM, Haroutunian V, Gabriel S, Knott PJ, Carlin LS, Purohit DP, Perl DP, Schmeidler J, Kanof P, Davis KL, 1995 Neurochemical correlates of dementia severity in Alzheimer's disease: relative importance of the cholinergic deficits. *J. Neurochem.* 64, 749–760. <http://dx.doi.org/10.1046/j.1471-4159.1995.64020749.x>. [PubMed: 7830069]
- Bondareff W, Mountjoy CQ, Roth M, Rossor MN, Iversen LL, Reynolds GP, Hauser DL, 1987 Neuronal degeneration in locus ceruleus and cortical correlates of Alzheimer disease. *Alzheimer Dis. Assoc. Disord.* 1, 256–262. [PubMed: 3453748]
- Braak H, Braak E, 1991 Neuropathological staging of Alzheimer-related changes. *Acta Neuropathol.* 82 (4), 239–259. [PubMed: 1759558]
- Braak E, Braak H, Mandelkow EM, 1994 A sequence of cytoskeleton changes related to the formation of neurofibrillary tangles and neurofilament threads. *Acta Neuropathol.* 87, 554–567. [PubMed: 7522386]
- Breese CR, Adams C, Logel J, Drebing C, Rollins Y, Barnhart M, Sullivan B, Demasters BK, Freedman R, Leonard S, 1997 Comparison of the regional expression of nicotinic acetylcholine receptor alpha 7 mRNA and [I-125]alpha-bungarotoxin binding in human postmortem brain. *J. Comp. Neurol.* 387, 385–398. [PubMed: 9335422]
- Bruckner SR, Tammariello SP, Kuan CY, Flavell RA, Rakic P, Estus S, 2001 JNK3 contributes to c-Jun activation and apoptosis but not oxidative stress in nerve growth factor-deprived sympathetic neurons. *J. Neurochem.* 78, 298–303. [PubMed: 11461965]
- Buettner F, Natarajan KN, Casale FP, Proserpio V, Scialdone A, Theis FJ, Teichmann SA, Marioni JC, Stegle O, 2015 Computational analysis of cell-to-cell heterogeneity in single-cell RNA-sequencing data reveals hidden subpopulations of cells. *Nat. Biotechnol.* 33, 155–160. <http://dx.doi.org/10.1093/bioinformatics/bts385>. [PubMed: 25599176]
- Burgering B, Coffey PJ, 1995 Protein-kinase-B (C-Akt) in phosphatidylinositol-3-OH inase signal-transduction. *Nature* 376, 599–602. <http://dx.doi.org/10.1038/376599a0>. [PubMed: 7637810]
- Cao X, Cui Z, Feng R, Tang Y-P, Qin Z, Mei B, Tsien JZ, 2007 Maintenance of superior learning and memory function in NR2B transgenic mice during ageing. *Eur. J. Neurosci.* 25, 1815–1822. <http://dx.doi.org/10.1111/jphysiol.1996.sp021779>. [PubMed: 17432968]
- Carter BD, Kaltschmidt C, Kaltschmidt B, Offenhauser N, Bohm-Matthaei R, Baeuerle PA, Barde Y-A, 1996 Selective activation of NF-kappaB by nerve growth factor through the neurotrophin receptor p75. *Science* 272, 542. [PubMed: 8614802]
- Casaccia-Bonnel P, Carter BD, Dobrowsky RT, Chao MV, 1996 Death of oligodendrocytes mediated by the interaction of nerve growth factor with its receptor p75. *Nature* 383, 716–719. <http://dx.doi.org/10.1038/383716a0>. [PubMed: 8878481]
- Che S, Ginsberg SD, 2004 Amplification of RNA transcripts using terminal continuation. 84, 131–137. <http://dx.doi.org/10.1038/sj.labinvest.3700005>.

- Chen C, Li X, Wang T, Wang H-H, Fu Y, Zhang L, Xiao S-F, 1984 Association between NMDA receptor subunit 2b gene polymorphism and Alzheimer's disease in Chienes Han population in Shanghai. *Neurol. Sci* 34, 939–944. <http://dx.doi.org/10.1212/WNL.34.7.939>.
- Chu YP, Cochran EJ, Bennett DA, Mufson EJ, Kordower JH, 2001 Down-regulation of trkA mRNA within nucleus basalis neurons in individuals with mild cognitive impairment and Alzheimer's disease. *J. Comp. Neurol.* 437, 296–307. [PubMed: 11494257]
- Counts SE, Mufson EJ, 2005 The role of nerve growth factor receptors in cholinergic basal forebrain degeneration in prodromal Alzheimer disease. *J. Neuropathol. Exp. Neurol.* 64, 263–272. [PubMed: 15835262]
- Counts SE, Nadeem M, Wu J, Ginsberg SD, Saragovi HU, Mufson EJ, 2004 Reduction of cortical TrkA but not p75NTR protein in early-stage Alzheimer's disease. *Ann. Neurol.* 56, 520–531. <http://dx.doi.org/10.1002/ana.20233>. [PubMed: 15455399]
- Counts SE, Nadeem M, Lad SP, Wu J, Mufson EJ, 2006 Differential expression of synaptic proteins in the frontal and temporal cortex of elderly subjects with mild cognitive impairment. *J. Neuropathol. Exp. Neurol.* 65, 592–601. [PubMed: 16783169]
- Counts SE, He B, Che S, Ikonomic MD, DeKosky ST, Ginsberg SD, Mufson EJ, 2007 Alpha 7 nicotinic receptor up-regulation in cholinergic basal forebrain neurons in Alzheimer disease. *Arch. Neurol.* 64, 1771–1776. <http://dx.doi.org/10.1001/archneur.64.12.1771>. [PubMed: 18071042]
- Counts SE, Alldred MJ, Che S, Ginsberg SD, Mufson EJ, 2014 Synaptic dysregulation within hippocampal CA1 pyramidal neurons in mild cognitive impairment. *Neuropharmacology* 79, 172–179. <http://dx.doi.org/10.1016/j.neuropharm.2013.10.018>. [PubMed: 24445080]
- Datta K, Bellacosa A, Chan TO, Tsichlis PN, 1996 Akt is a direct target of the phosphatidylinositol 3-kinase - activation by growth factors, v-src and v-Ha-ras, in Sf9 and mammalian cells. *J. Biol. Chem.* 271, 30835–30839. [PubMed: 8940066]
- Dudek H, Datta SR, Franke TF, Birnbaum MJ, Yao R, Cooper GM, Segal RA, Kaplan DR, Greenberg ME, 1997 Regulation of neuronal survival by the serinethreonine protein kinase Akt. *Science* 275, 661–665. [PubMed: 9005851]
- Eilers A, Whitfield J, Shah B, Spadoni C, Desmond H, Ham J, 2001 Direct inhibition of c-Jun N-terminal kinase in sympathetic neurones prevents c-jun promoter activation and NGF withdrawal-induced death. *J. Neurochem.* 76, 1439–1454. [PubMed: 11238729]
- Farber NB, Newcomer JW, Olney JW, 1998 The glutamate synapse in neuropsychiatric disorders: focus on schizophrenia and Alzheimer's disease. *Prog. Brain Res.* 116, 421–437. [PubMed: 9932393]
- Frade JM, Rodriguez-Tebar A, Barde YA, 1996 Induction of cell death by endogenous nerve growth factor through its p75 receptor. *Nature* 383, 166–168. <http://dx.doi.org/10.1038/383166a0>. [PubMed: 8774880]
- Franke TF, Kaplan DR, Cantley LC, Toker A, 1997 Direct regulation of the Akt proto-oncogene product by phosphatidylinositol-3,4-bisphosphate. *Science* 275, 665–668. [PubMed: 9005852]
- Friedman WJ, 2000 Neurotrophins induce death of hippocampal neurons via the p75 receptor. *J. Neurosci.* 20, 6340–6346. [PubMed: 10964939]
- Gamblin TC, Chen F, Zambrano A, Abraha A, Lagalwar S, Guillozet AL, Lu M, Fu Y, García-Sierra F, LaPointe N, Miller R, Berry RW, Binder LI, Cryns VL, 2003 Caspase cleavage of tau: linking amyloid and neurofibrillary tangles in Alzheimer's disease. *PNAS* 100, 10032–10037. <http://dx.doi.org/10.1073/pnas.1630428100>. [PubMed: 12888622]
- García-Sierra F, Ghoshal N, Quinn B, Berry RW, Binder LI, 2003 Conformational changes and truncation of tau protein during tangle evolution in Alzheimer's disease. *J. Alzheimers Dis.* 5, 65–77. [PubMed: 12719624]
- Gentry JJ, Casaccia-Bonnel P, Carter BD, 2000 Nerve growth factor activation of nuclear factor κ B through its p75 receptor is an anti-apoptotic signal in RN22 schwannoma cells. *J. Biol. Chem.* 275, 7558–7565. [PubMed: 10713062]
- Ghoshal N, Garcia-Sierra F, Fu YF, Beckett LA, Mufson EJ, Kuret J, Berry RW, Binder LI, 2001 Tau-66: evidence for a novel tau conformation in Alzheimer's disease. *J. Neurochem.* 77, 1372–1385. [PubMed: 11389188]

- Ghoshal N, García-Sierra F, Wu J, Leurgans S, Bennett DA, Berry RW, Binder LI, 2002 Tau conformational changes correspond to impairments of episodic memory in mild cognitive impairment and Alzheimer's disease. *Exp. Neurol.* 177, 475–493. <http://dx.doi.org/10.1006/exnr.2002.8014>. [PubMed: 12429193]
- Gibb WR, Mountjoy CQ, Mann DM, Lees AJ, 1989 The substantia nigra and ventral tegmental area in Alzheimer's disease and Down's syndrome. *J. Neurol. Neurosurg. Psychiatry* 52, 193–200. [PubMed: 2539435]
- Ginsberg SD, 2005 RNA amplification strategies for small sample populations. *Methods* 37, 229–237. <http://dx.doi.org/10.1016/j.ymeth.2005.09.003>. [PubMed: 16308152]
- Ginsberg SD, Crino PB, Lee VM, Eberwine JH, Trojanowski JQ, 1997 Sequestration of RNA in Alzheimer's disease neurofibrillary tangles and senile plaques. *Ann. N.Y. Acad. Sci.* 41, 200–209. <http://dx.doi.org/10.1002/ana.410410211>.
- Ginsberg SD, Che S, Wu J, Counts SE, Mufson EJ, 2006 Down regulation of *trk* but not *p75^{NTR}* gene expression in single cholinergic basal forebrain neurons mark the progression of Alzheimer's disease. *J. Neurochem.* 97, 475–487. <http://dx.doi.org/10.1111/j.1471-4159.2006.03764.x>. [PubMed: 16539663]
- Ginsberg SD, Alldred MJ, Counts SE, Cataldo AM, Neve RL, Jiang Y, Wu J, Chao MV, Mufson EJ, Nixon RA, Che S, 2010a Microarray analysis of hippocampal CA1 neurons implicates early endosomal dysfunction during Alzheimer's disease progression. *Biol. Psychiatry* 68, 885–893. <http://dx.doi.org/10.1016/j.biopsych.2010.05.030>. [PubMed: 20655510]
- Ginsberg SD, Mufson EJ, Counts SE, Wu J, Alldred MJ, Nixon RA, Che S, 2010b Regional selectivity of *rab5* and *rab7* protein upregulation in mild cognitive impairment and Alzheimer's disease. *J. Alzheimers Dis.* 22, 631–639. <http://dx.doi.org/10.3233/JAD-2010-101080>. [PubMed: 20847427]
- Ginsberg SD, Alldred MJ, Che S, 2012 Gene expression levels assessed by CA1 pyramidal neuron and regional hippocampal dissections in Alzheimer's disease. *Neurobiol. Dis.* 45, 99–107. <http://dx.doi.org/10.1016/j.nbd.2011.07.013>. [PubMed: 21821124]
- Ginsberg SD, Malek-Ahmadi MH, Alldred MJ, Che S, Elarova I, Chen Y, Jeanneteau F, Kranz TM, Chao MV, Counts SE, Mufson EJ, 2017 Selective decline of neurotrophin and neurotrophin receptor genes within CA1 pyramidal neurons and hippocampus proper: correlation with cognitive performance and neuropathology in mild cognitive impairment and Alzheimer's disease. *Hippocampus*. <http://dx.doi.org/10.1002/hipo.22802>.
- Gotti C, Fornasari D, Clementi F, 1997 Human neuronal nicotinic receptors. *Prog. Neurobiol.* 53, 199–237. [PubMed: 9364611]
- Gross A, Jockel J, Wei MC, Korsmeyer SJ, 1998 Enforced dimerization of BAX results in its translocation, mitochondrial dysfunction and apoptosis. *EMBO J.* 17, 3878–3885. <http://dx.doi.org/10.1093/emboj/17.14.3878>. [PubMed: 9670005]
- Guillozet-Bongaarts AL, García-Sierra F, Reynolds MR, Horowitz PM, Fu Y, Wang T, Cahill ME, Bigio EH, Berry RW, Binder LI, 2005 Tau truncation during neurofibrillary tangle evolution in Alzheimer's disease. *Neurobiol. Aging* 26, 1015–1022. <http://dx.doi.org/10.1016/j.neurobiolaging.2004.09.019>. [PubMed: 15748781]
- Guillozet-Bongaarts AL, Cahill ME, Cryns VL, Reynolds MR, Berry RW, Binder LI, 2006 Pseudophosphorylation of tau at serine 422 inhibits caspase cleavage: in vitro evidence and implications for tangle formation in vivo. *J. Neurochem.* 97, 1005–1014. <http://dx.doi.org/10.1111/j.1471-4159.2006.03784.x>. [PubMed: 16606369]
- Harding TC, Xue L, Bienemann A, Haywood D, Dickens M, Tolkovsky AM, Uney JB, 2001 Inhibition of JNK by overexpression of the JNK binding domain of JIP-1 prevents apoptosis in sympathetic neurons. *J. Biol. Chem.* 276, 4531–4534. <http://dx.doi.org/10.1074/jbc.C000815200>. [PubMed: 11121395]
- Hellström-Lindahl E, Mousavi M, Zhang X, Ravid R, Nordberg A, 1999 Regional distribution of nicotinic receptor subunit mRNAs in human brain: comparison between Alzheimer and normal brain. *Brain Res. Mol. Brain Res.* 66, 94–103. [PubMed: 10095081]
- Hempstead BL, Martin-Zanca D, Kaplan DR, Parada LF, Chao MV, 1991 Highaffinity NGF binding requires coexpression of the *trk* proto-oncogene and the lowaffinity NGF receptor. *Nature* 350, 678–683. <http://dx.doi.org/10.1038/350678a0>. [PubMed: 1850821]

- Hollmann M, Hartley M, Heinemann S, 1991 Ca²⁺ permeability of KAAMPA—gated glutamate receptor channels depends on subunit composition. *Science* 252, 851–853. [PubMed: 1709304]
- Holtzman DM, Li Y, Parada LF, Kinsman S, Chen CK, Valletta JS, Zhou J, Long JB, Mobley WC, 1992 p140trk mRNA marks NGF-responsive forebrain neurons: evidence that trk gene expression is induced by NGF. *Neuron* 9, 465–478. [PubMed: 1524827]
- Hu N-W, Ondrejcek T, Rowan MJ, 2012 Glutamate receptors in preclinical research on Alzheimer's disease: Update on recent advances. *Pharmacol. Biochem. Behav.* 100, 855–862. <http://dx.doi.org/10.1016/j.pbb.2011.04.013>. [PubMed: 21536064]
- Hyman BT, Phelps CH, Beach TG, Bigio EH, Cairns NJ, Carrillo MC, Dickson DW, Duyckaerts C, Frosch MP, Masliah E, Mirra SS, Nelson PT, Schneider JA, Thal DR, Thies B, Trojanowski JQ, Vinters HV, Montine TJ, 2012 National Institute on Aging–Alzheimer's Association guidelines for the neuropathologic assessment of Alzheimer's disease. *Alzheimers Dement.* 8, 1–13. <http://dx.doi.org/10.1016/j.jalz.2011.10.007>. [PubMed: 22265587]
- Jones BE, Cuello AC, 1989 Afferents to the basal forebrain cholinergic cell area from pontomesencephalic–catecholamine, serotonin, and acetylcholine–neurons. *Neuroscience* 31, 37–61. [PubMed: 2475819]
- Kanaan NM, Kordower JH, Collier TJ, 2007 Age-related accumulation of Marinesco bodies and lipofuscin in rhesus monkey midbrain dopamine neurons: relevance to selective neuronal vulnerability. *J. Comp. Neurol.* 502, 683–700. <http://dx.doi.org/10.1002/cne.21333>. [PubMed: 17436290]
- Kanaan NM, Kordower JH, Collier TJ, 2010 Age-related changes in glial cells of dopamine midbrain subregions in rhesus monkeys. *Neurobiol. Aging* 31, 937–952. <http://dx.doi.org/10.1016/j.neurobiolaging.2008.07.006>. [PubMed: 18715678]
- Kanaan NM, Morfini GA, LaPointe NE, Pigino GF, Patterson KR, Song Y, Andreadis A, Fu Y, Brady ST, Binder LI, 2011 Pathogenic forms of tau inhibit kinesin-dependent axonal transport through a mechanism involving activation of axonal phosphotransferases. *J. Neurosci.* 31, 9858–9868. <http://dx.doi.org/10.1523/JNEUROSCI.0560-11.2011>. [PubMed: 21734277]
- Kanaan NM, Morfini G, Pigino G, LaPointe NE, Andreadis A, Song Y, Leitman E, Binder LI, Brady ST, 2012 Phosphorylation in the amino terminus of tau prevents inhibition of anterograde axonal transport. *Neurobiol. Aging* 33, 826.e15–826.e30. <http://dx.doi.org/10.1016/j.neurobiolaging.2011.06.006>.
- Kaplan DR, Miller FD, 2000 Neurotrophin signal transduction in the nervous system. *Curr. Opin. Neurobiol.* 10, 381–391. [PubMed: 10851172]
- Kelly SC, He Bin, Perez SE, Ginsberg SD, Mufson EJ, Counts SE, 2017 Locus coeruleus cellular and molecular pathology during the progression of. *Acta Neuropathol. Commun.* 1–14. <http://dx.doi.org/10.1186/s40478-017-0411-2>. [PubMed: 28057070]
- Kendziorra K, Wolf H, Meyer PM, Barthel H, Hesse S, Becker GA, Luthardt J, Schildan A, Patt M, Sorger D, Seese A, Gertz H-J, Sabri O, 2010 Decreased cerebral $\alpha 4\beta 2^*$ nicotinic acetylcholine receptor availability in patients with mild cognitive impairment and Alzheimer's disease assessed with positron emission tomography. *Eur. J. Nucl. Med. Mol. Imaging* 38, 515–525. <http://dx.doi.org/10.1007/s00259-010-1644-5>.
- Kim T, Lim C-S, Kaang B-K, 2015 Cell type-specific gene expression profiling in brain tissue: comparison between TRAP, LCM and RNA-seq. *BMB Rep* 48, 388–394. <http://dx.doi.org/10.5483/BMBRep.2015.48.7.218>. [PubMed: 25603796]
- Klesse LJ, Parada LF, 1999 Trks: signal transduction and intracellular pathways. *Microsc. Res. Tech.* 45, 210–216. [http://dx.doi.org/10.1002/\(SICI\)1097-0029\(19990515/01\)45:4/5<210::AID-JEMT4>3.0.CO;2-F](http://dx.doi.org/10.1002/(SICI)1097-0029(19990515/01)45:4/5<210::AID-JEMT4>3.0.CO;2-F). [PubMed: 10383113]
- Klippel A, Reinhard C, Kavanaugh WM, Apell G, Escobedo M, Williams LT, 1996 Membrane localization of phosphatidylinositol 3-kinase is sufficient to activate multiple signal-transducing kinase pathways. *Mol. Cell. Biol.* 16, 4117–4127. [PubMed: 8754810]
- Lad SP, Neet KE, Mufson EJ, 2003 Nerve growth factor: structure, function and therapeutic implications for Alzheimer's disease. *Curr. Drug Targets CNS Neurol. Disord* 2, 315–334. [PubMed: 14529363]

- LaPointe NE, Morfini G, Pigino G, Gaisina IN, Kozikowski AP, Binder LI, Brady ST, 2009 The amino terminus of tau inhibits kinesin-dependent axonal transport: implications for filament toxicity. *J. Neurosci. Res.* 87, 440–451. <http://dx.doi.org/10.1002/jnr.21850>. [PubMed: 18798283]
- Levey AI, 1996 Muscarinic acetylcholine receptor expression in memory circuits: implications for treatment of Alzheimer disease. *PNAS* 93, 13541–13546. [PubMed: 8942969]
- Li YW, Holtzman DM, Kromer LF, Kaplan DR, Chuacouzens J, Clary DO, Knusel B, Mobley WC, 1995 Regulation of Trka and Chat expression in developing rat basal forebrain - evidence that both exogenous and endogenous Ngf regulate differentiation of cholinergic neurons. *J. Neurosci.* 15, 2888–2905. [PubMed: 7536822]
- Macosko EZ, Basu A, Satija R, Nemes J, Shekhar K, Goldman M, Tirosh I, Bialas AR, Kamitaki N, Martersteck EM, Trombetta JJ, Weitz DA, Sanes JR, Shalek AK, Regev A, McCarroll SA, 2015 Highly parallel genome-wide expression profiling of individual cells using nanoliter droplets. *Cell* 161, 1202–1214. <http://dx.doi.org/10.1016/j.cell.2015.05.002>. [PubMed: 26000488]
- Mahadeo D, Kaplan L, Chao MV, Hempstead BL, 1994 High affinity nerve growth factor binding displays a faster rate of association than p140trk binding. Implications for multi-subunit polypeptide receptors. *J. Biol. Chem.* 269, 6884–6891. [PubMed: 8120051]
- Mamidipudi V, Wooten MW, 2002 Dual role for p75NTR signaling in survival and cell death: can intracellular mediators provide an explanation? *J. Neurosci. Res.* 68, 373–384. <http://dx.doi.org/10.1002/jnr.10244>. [PubMed: 11992464]
- Mann DM, Lincoln J, Yates PO, Stamp JE, Toper S, 1980 Changes in the monoamine containing neurones of the human CNS in senile dementia. *Br. J. Psychiatry* 136, 533–541. [PubMed: 6155966]
- Martin DP, Schmidt RE, Distefano PS, Lowry OH, Carter JG, Johnson EM, 1988 Inhibitors of protein-synthesis and RNA-synthesis prevent neuronal death caused by nerve growth-factor deprivation. *J. Cell Biol.* 106, 829–844. [PubMed: 2450099]
- Martinou I, Desagher S, Eskes R, Antonsson B, Andre E, Fakan S, Martinou J, 1999 The release of cytochrome c from mitochondria during apoptosis of NGF-deprived sympathetic neurons is a reversible event. *J. Cell Biol.* 144, 883–889. [PubMed: 10085288]
- Masoudi R, Ioannou MS, Coughlin MD, Pagadala P, Neet KE, Clewes O, Allen SJ, Dawbarn D, Fahnestock M, 2009 Biological activity of nerve growth factor precursor is dependent upon relative levels of its receptors. *J. Biol. Chem.* 284, 18424–18433. <http://dx.doi.org/10.1074/jbc.M109.007104>. [PubMed: 19389705]
- Mesulam M, Mufson EJ, Levey AI, Wainer BH, 1983 Cholinergic innervation of cortex by the basal forebrain: cytochemistry and cortical connections of the septal area, diagonal band nuclei, nucleus basalis (substantia innominata), and hypothalamus in the rhesus monkey. *J. Comp. Neurol.* 214, 170–197. [PubMed: 6841683]
- Mesulam M, Shaw P, Mash D, Weintraub S, 2004 Cholinergic nucleus basalis tauopathy emerges early in the aging-MCI-AD continuum. *Ann. Neurol.* 55, 815–828. <http://dx.doi.org/10.1002/ana.20100>. [PubMed: 15174015]
- Miller FD, Kaplan DR, 2001 Neurotrophin signalling pathways regulating neuronal apoptosis. *Cell. Mol. Life Sci.* 58, 1045–1053. <http://dx.doi.org/10.1007/PL00000919>. [PubMed: 11529497]
- Mirra SS, Heyman A, McKeel D, Sumi SM, Crain BJ, 1991 The Consortium to Establish a Registry for Alzheimer's Disease (CERAD) part II. Standardization of the neuropathologic assessment of Alzheimer's disease. *Neurol. Sci.* 41, 479–486.
- Mufson EJ, Bothwell M, Hersh LB, Kordower JH, 1989 Nerve growth factor receptor immunoreactive profiles in the normal, aged human basal forebrain: colocalization with cholinergic neurons. *J. Comp. Neurol.* 285, 196–217. <http://dx.doi.org/10.1002/cne.902850204>. [PubMed: 2547849]
- Mufson EJ, Conner JM, Kordower JH, 1995 Nerve growth-factor in Alzheimersdisease: defective retrograde transport to nucleus basalis. *Neuroreport* 6, 1063–1066. [PubMed: 7632896]
- Mufson EJ, Lavine N, Kordower JH, Quirion R, Saragovi HU, 1997 Reduction in p140-TrkA receptor protein within the nucleus basalis and cortex in Alzheimer's disease. *Exp. Neurol.* 146, 91–103. [PubMed: 9225742]

- Mufson EJ, Jaffar S, Levey AI, 1998 m2 muscarinic acetylcholine receptor-immunoreactive neurons are not reduced within the nucleus basalis in Alzheimer's disease: relationship with cholinergic and *J. Comp. Neurol.* 392, 313–329. [PubMed: 9511920]
- Mufson EJ, Chen EY, Cochran EJ, Beckett LA, Bennett DA, Kordower JH, 1999 Entorhinal cortex β -amyloid load in individuals with mild cognitive impairment. *Exp. Neurol.* 158, 469–490. [PubMed: 10415154]
- Mufson EJ, Ma SY, Cochran EJ, Bennett DA, Beckett LA, Jaffar S, Saragovi HU, Kordower JH, 2000 Loss of nucleus basalis neurons containing trkA immunoreactivity in individuals with mild cognitive impairment and early Alzheimer's disease. *J. Comp. Neurol.* 427, 19–30. [http://dx.doi.org/10.1002/1096-9861\(20001106\)427:1<19::AID-CNE2>3.0.CO;2-A](http://dx.doi.org/10.1002/1096-9861(20001106)427:1<19::AID-CNE2>3.0.CO;2-A). [PubMed: 11042589]
- Mufson EJ, Counts SE, Ginsberg SD, 2002a Gene expression profiles of cholinergic nucleus basalis neurons in Alzheimer's disease. *Neurochem. Res.* 27, 1035–1048. [PubMed: 12462403]
- Mufson EJ, Ma SY, Dills J, Cochran EJ, Leurgans S, Wu J, Bennett DA, Jaffar S, Gilmor ML, Levey AI, Kordower JH, 2002b Loss of basal forebrain P75NTR immunoreactivity in subjects with mild cognitive impairment and Alzheimer's disease. *J. Comp. Neurol.* 443, 136–153. <http://dx.doi.org/10.1002/cne.10122>. [PubMed: 11793352]
- Mufson EJ, Ginsberg SD, Ikonovic MD, DeKosky ST, 2003 Human cholinergic basal forebrain: chemoanatomy and neurologic dysfunction. *J. Chem. Neuroanat.* 26, 233–242. [http://dx.doi.org/10.1016/S0891-0618\(03\)00068-1](http://dx.doi.org/10.1016/S0891-0618(03)00068-1). [PubMed: 14729126]
- Mufson EJ, Counts SE, Fahnstock M, Ginsberg SD, 2007 Cholinergic molecular substrates of mild cognitive impairment in the elderly. *Curr. Alzheimer Res.* 4, 340–350. [PubMed: 17908035]
- Mufson EJ, Malek-Ahmadi M, Snyder N, Ausdemore J, Chen K, Perez SE, 2016 Braak stage and trajectory of cognitive decline in noncognitively impaired elders. *Neurobiol. Aging* 43, 101–110. <http://dx.doi.org/10.1016/j.neurobiolaging.2016.03.003>. [PubMed: 27255819]
- Nishizuka Y, 1988 The molecular heterogeneity of protein kinase C and its implications for cellular regulation. *Nature* 334, 661–665. [PubMed: 3045562]
- Olney JW, Wozniak DF, Farber NB, 1997 Excitotoxic neurodegeneration in Alzheimer disease. New hypothesis and new therapeutic strategies. *Arch. Neurol.* 54, 1234–1240. [PubMed: 9341569]
- Park DS, Levine B, Ferrari G, Greene LA, 1997 Cyclin dependent kinase inhibitors and dominant negative cyclin dependent kinase 4 and 6 promote survival of NGFdeprived sympathetic neurons. *J. Neurosci.* 17, 8975–8983. [PubMed: 9364045]
- Park DS, Morris EJ, Padmanabhan J, Shelanski ML, Geller HM, Greene LA, 1998 Cyclin-dependent kinases participate in death of neurons evoked by DNA-damaging agents. *J. Cell Biol.* 143, 457–467. [PubMed: 9786955]
- Park DS, Morris EJ, Bremner R, Keramaris E, Padmanabhan J, Rosenbaum M, Shelanski ML, Geller HM, Greene LA, 2000 Involvement of retinoblastoma family members and E2F/DP complexes in the death of neurons evoked by DNA damage. *J. Neurosci.* 20, 3104–3114. [PubMed: 10777774]
- Peng SY, Wu J, Mufson EJ, Fahnstock M, 2004 Increased proNGF levels in subjects with mild cognitive impairment and mild Alzheimer disease. *J. Neuropathol. Exp. Neurol.* 63, 641–649. [PubMed: 15217092]
- Perez SE, He B, Nadeem M, Wu J, Ginsberg SD, Ikonovic MD, Mufson EJ, 2015a Hippocampal endosomal, lysosomal, and autophagic dysregulation in mild cognitive impairment: correlation with A β and tau pathology. *J. Neuropathol. Exp. Neurol.* 74.
- Perez SE, He B, Nadeem M, Wu J, Scheff SW, Abrahamson EE, Ikonovic MD, Mufson EJ, 2015b Resilience of precuneus neurotrophic signaling pathways despite amyloid pathology in prodromal Alzheimer's disease. *Biol. Psychiatry* 77, 693–703. <http://dx.doi.org/10.1016/j.biopsych.2013.12.016>. [PubMed: 24529280]
- Petersen RC, Doody R, Kurz A, Mohs RC, Morris JC, Rabins PV, Ritchie K, Rosser M, Thal L, Winblad B, 2001 Current concepts in mild cognitive impairment. *Arch. Neurol.* 58, 1985–1992. <http://dx.doi.org/10.1001/archneur.58.12.1985>. [PubMed: 11735772]
- Putcha GV, Deshmukh M, Johnson EM, 1999 BAX translocation is a critical event in neuronal apoptosis: regulation by neuroprotectants, BCL-2, and caspases. *J. Neurosci.* 19, 7476–7485. [PubMed: 10460254]

- Reiner A, Yekutieli D, Benjamini Y, 2003 Identifying differentially expressed genes using false discovery rate controlling procedures. *19*, 368–375. <http://dx.doi.org/10.1093/bioinformatics/btf877>.
- Riascos D, Nicholas A, Samaeekia R, Yukhananov R, Mesulam MM, Bigio EH, Weintraub S, Guo L, Geula C, 2014 Neurobiology of aging. *Neurobiol. Aging* 35, 1325–1333. <http://dx.doi.org/10.1016/j.neurobiolaging.2013.12.017>. [PubMed: 24461366]
- Roux PP, Barker PA, 2002 Neurotrophin signaling through the p75 neurotrophin receptor. *Prog. Neurobiol.* 67, 203–233. [PubMed: 12169297]
- Roux PP, Bhakar AL, Kennedy TE, Barker PA, 2001 The p75 neurotrophin receptor activates Akt (protein kinase B) through a phosphatidylinositol 3-kinase-dependent pathway. *J. Biol. Chem.* 276, 23097–23104. <http://dx.doi.org/10.1074/jbc.M011520200>. [PubMed: 11312266]
- Salehi A, Verhaagen J, Dijkhuizen PA, Swaab DF, 1996 Co-localization of highaffinity neurotrophin receptors in nucleus basalis of Meynert neurons and their differential reduction in Alzheimer's disease. *Neuroscience* 75, 373–387. [PubMed: 8931004]
- Scott SA, Mufson EJ, Weingarten JA, Skau KA, Crutcher KA, 1995 Nerve growth-factor in Alzheimers-disease: increased levels throughout the brain coupled with declines in nucleus basalis. *J. Neurosci.* 15, 6213–6221. [PubMed: 7666203]
- Smiley JF, Mesulam MM, 1999 Cholinergic neurons of the nucleus basalis of meynert receive cholinergic, catecholaminergic and gabaergic synapses: an electron microscopic investigation in the monkey. *Neuroscience* 88, 241–255. [PubMed: 10051204]
- Smiley JF, Subramanian M, Mesulam MM, 1999 Monoaminergic-cholinergic interactions in the primate basal forebrain. *Neuroscience* 93, 817–829. [PubMed: 10473248]
- Sofroniew MV, Howe CL, Mobley WC, 2001 Nerve growth factor signaling, neuroprotection, and neural repair. *Annu. Rev. Neurosci.* 24, 1217–1281. [PubMed: 11520933]
- Sze CI, Bi H, Kleinschmidt-DeMasters BK, Filley CM, Martin LJ, 2001 N-methyl-D-aspartate receptor subunit proteins and their phosphorylation status are altered selectively in Alzheimer's disease. *J. Neurol. Sci.* 182, 151–159. [PubMed: 11137521]
- Tang YP, Wang H, Feng R, Kyin M, Tsien JZ, 2001 Differential effects of enrichment on learning and memory function in NR2B transgenic mice. *Neuropharmacology* 41, 779–790. [PubMed: 11640933]
- Teaktong T, Graham AJ, Court JA, Perry RH, Jaros E, Johnson M, Hall R, Perry EK, 2004 Nicotinic acetylcholine receptor immunohistochemistry in Alzheimer's disease and dementia with Lewy bodies: differential neuronal and astroglial pathology. *J. Neurol. Sci.* 225, 39–49. <http://dx.doi.org/10.1016/j.jns.2004.06.015>. [PubMed: 15465084]
- Terrière E, Dempsey MF, Herrmann LL, Tierney KM, Lonie JA, O'Carroll RE, Pimlott S, Wyper DJ, Herholz K, Ebmeier KP, 2010 5-¹²³I-A-85380 binding to the α 4 β 2-nicotinic receptor in mild cognitive impairment. *Neurobiol. Aging* 31, 1885–1893. <http://dx.doi.org/10.1016/j.neurobiolaging.2008.10.008>. [PubMed: 19036475]
- Theofilas P, Ehrenberg AJ, Dunlop S, Di Lorenzo Alho AT, Nguy A, Leite REP, Rodriguez RD, Mejia MB, Suemoto CK, Ferretti-Rebustini REDL, Polichiso L, Nascimento CF, Seeley WW, Nitrini R, Pasqualucci CA, Jacob Filho W, Rueb U, Neuhaus J, Heinsen H, Grinberg LT, 2017 Locus coeruleus volume and cell population changes during Alzheimer's disease progression: a stereological study in human postmortem brains with potential implication for early-stage biomarker discovery. *Alzheimers Dement.* 13, 236–246. <http://dx.doi.org/10.1016/j.jalz.2016.06.2362>. [PubMed: 27513978]
- Tiernan CT, Combs B, Cox K, Morfini G, Brady ST, Counts SE, Kanaan NM, 2016a Pseudophosphorylation of tau at S422 enhances SDS-stable dimer formation and impairs both anterograde and retrograde fast axonal transport. *Exp. Neurol.* 283, 318–329. <http://dx.doi.org/10.1016/j.expneurol.2016.06.030>. [PubMed: 27373205]
- Tiernan CT, Ginsberg SD, Guillozet-Bongaarts AL, Ward SM, He Bin, Kanaan NM, Mufson EJ, Binder LI, Counts, 2016b Protein homeostasis gene dysregulation in pretangle-bearing nucleus basalis neurons during the progression of Alzheimer's disease. *Neurobiol. Aging* 42, 80–90. <http://dx.doi.org/10.1016/j.neurobiolaging.2016.02.031>. [PubMed: 27143424]

- Vana L, Kanaan NM, Ugwu IC, Wu J, Mufson EJ, Binder LI, 2011 Progression of tau pathology in cholinergic basal forebrain neurons in mild cognitive impairment and Alzheimer's disease. *Am. J. Pathol.* 179, 2533–2550. <http://dx.doi.org/10.1016/j.ajpath.2011.07.044>. [PubMed: 21945902]
- Wu C-K, Thal L, Pizzo D, Hansen L, Masliah E, Geula C, 2005 Apoptotic signals within the basal forebrain cholinergic neurons in Alzheimer's disease. *Exp. Neurol.* 195, 484–496. <http://dx.doi.org/10.1016/j.expneurol.2005.06.020>. [PubMed: 16085017]
- Yoon SO, Casaccia-Bonnel P, Carter B, Chao MV, 1998 Competitive signaling between TrkA and p75 nerve growth factor receptors determines cell survival. *J. Neurosci.* 18, 3273–3281. [PubMed: 9547236]
- Zaborszky L, Cullinan WE, 1996 Direct catecholaminergic-cholinergic interactions in the basal forebrain. I. Dopamine- β -hydroxylase-and tyrosine hydroxylase input to cholinergic neurons. *J. Comp. Neurol.* 374, 535–554. [PubMed: 8910734]

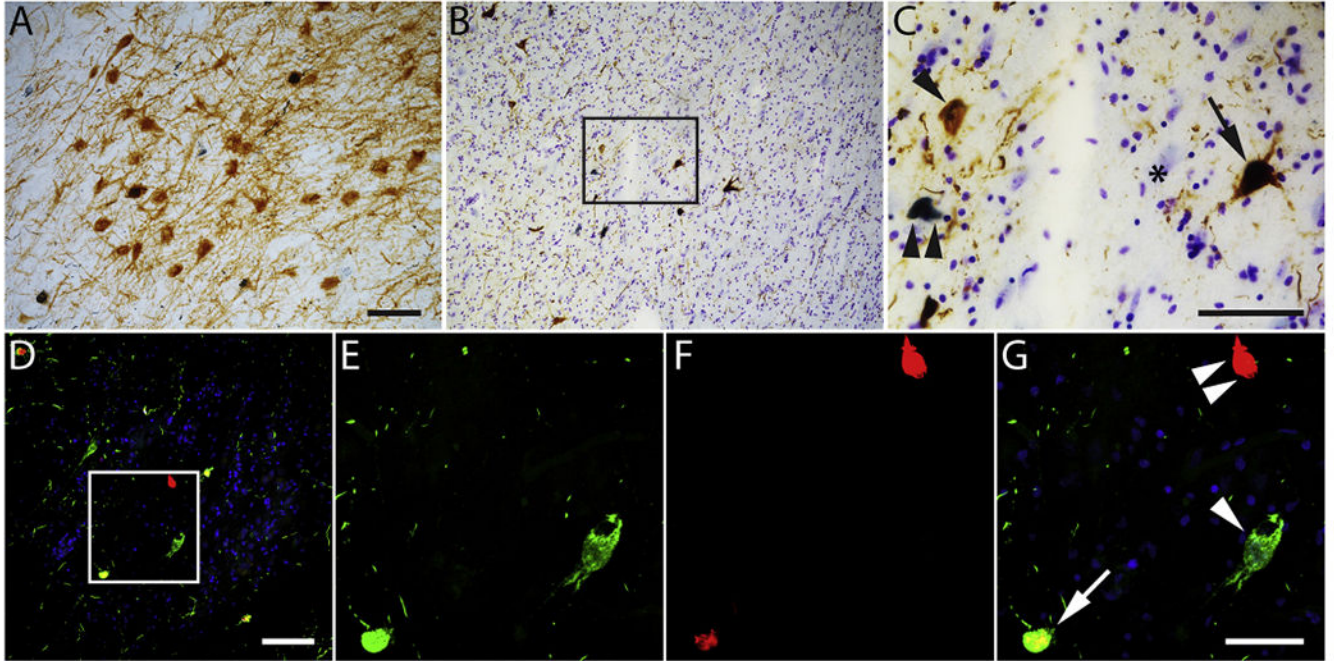


Fig. 1. Phenotypic characterization of NFT evolution with pS422 and TauC3 immunoreactivity in nbM neurons. (A–G) Tissue sections from the nbM of a representative AD case. (A) Cholinergic neurons in the nbM can be identified phenotypically by expression of the pan-neurotrophin (p75^{NTR}) receptor. A tissue section from a consecutive series was immunostained with p75^{NTR} (brown) and pS422 (blue) to confirm the location of the cholinergic nbM. (B) Low magnification view of the nbM subfield immunostained with pS422 (brown) and TauC3 (blue). (C) High magnification of pS422 and TauC3 pathology in boxed area from (B). A Nissl counterstain was used to identify nbM neurons lacking tau pathology (*). (D–G) Confocal microscopy was used to confirm the presence of three discrete populations of nbM neurons. (D) Low magnification view of nbM subfield. (E–G) High magnification of boxed area from (D) identify pS422 (E), TauC3 (F), and overlay (G). Single arrowhead indicates a pS422+ nbM neuron, double arrowheads indicate a TauC3+ nbM neuron, and arrow indicates a pS422+/TauC3+ nbM neuron (colocalization appears yellow). Scale bar in A, 100 μ m for A–B; scale bar in C, 50 μ m for C; scale bar in D, 100 μ m for D; scale bar in G, 50 μ m for E–G.

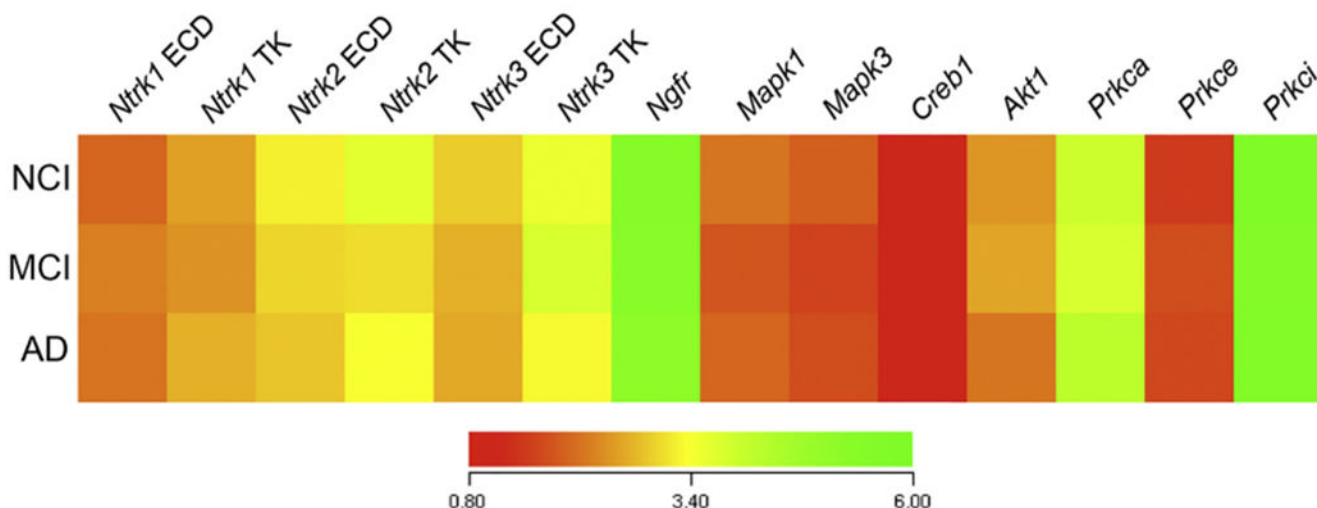


Fig. 2.

The expression of neurotrophin receptor and select downstream signaling molecule gene transcripts is equivalent in pS422+ nbM neurons during the progression of AD. Color-coded heatmap of the relative expression profiles for select transcripts in pS422+ nbM neurons aspirated from NCI, MCI, and AD cases (red to green = increasing mRNA levels).

Quantitative analysis revealed no statistical differences in the expression levels of the transcripts examined in pS422+ nbM neurons derived from MCI or AD compared to NCI. This observation suggests that the pathological state of the neuron, not disease status, may drive changes in gene expression. Therefore, in the present analysis, we compared mRNA levels in individual pS422+, pS422+/TauC3+, and TauC3+ nbM neurons independent of clinical diagnosis. Abbreviations: *Nrtk1*, *Nrtk2*, and *Nrtk3*, neurotrophin tyrosine kinase receptor type 1 (TrkA), 2 (TrkB), 3 (TrkC); ECD, extracellular domain; TK, intracellular tyrosine kinase domain; *Ngfr*, nerve growth factor receptor (p75^{NTR}); *Mapk1*, mitogen-activated protein kinase 1 (extracellular signal-regulated kinase 2); *Mapk3*, mitogen-activated protein kinase 3 (extracellular signal-regulated kinase 1); *Creb1*, cAMP response element binding protein; *Akt1*, Akt serine/threonine kinase 1 (protein kinase B); *Prkca*, *Prkce*, *Prkci*, protein kinase C alpha, epsilon, iota.

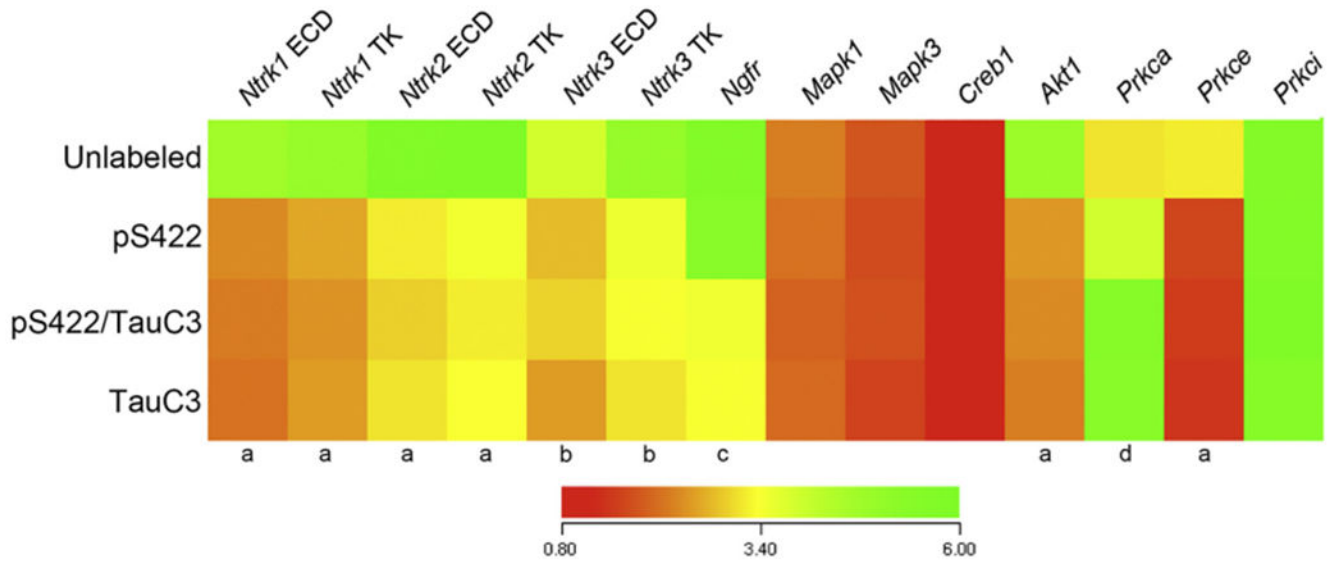


Fig. 3.

Neurotrophin receptor and select downstream signaling molecule mRNAs are dysregulated during the progression of NFT maturation. Heatmap of relative mRNA expression levels of neurotrophin receptors and downstream signaling molecules in pS422+, pS422+/TauC3+, and TauC3+ nbM neurons compared to unlabeled nbM neurons (red to green = increasing mRNA levels). Quantitative analysis revealed downregulated expression of *Ntrk1-3* transcripts as well as *Akt1* and *Prkce* in pS422+ nbM neurons as compared to unlabeled control neurons. Appearance of the late stage neopeptide TauC3 was associated with downregulation of the *Ngfr* transcript and upregulation of the *Prkca* transcript. a, unlabeled > pS422, $p < 0.001$; b, unlabeled > pS422, $p < 0.01$; c, pS422 > pS422+/TauC3+, $p < 0.01$; d, pS422 < pS422+/TauC3+, $p < 0.01$.

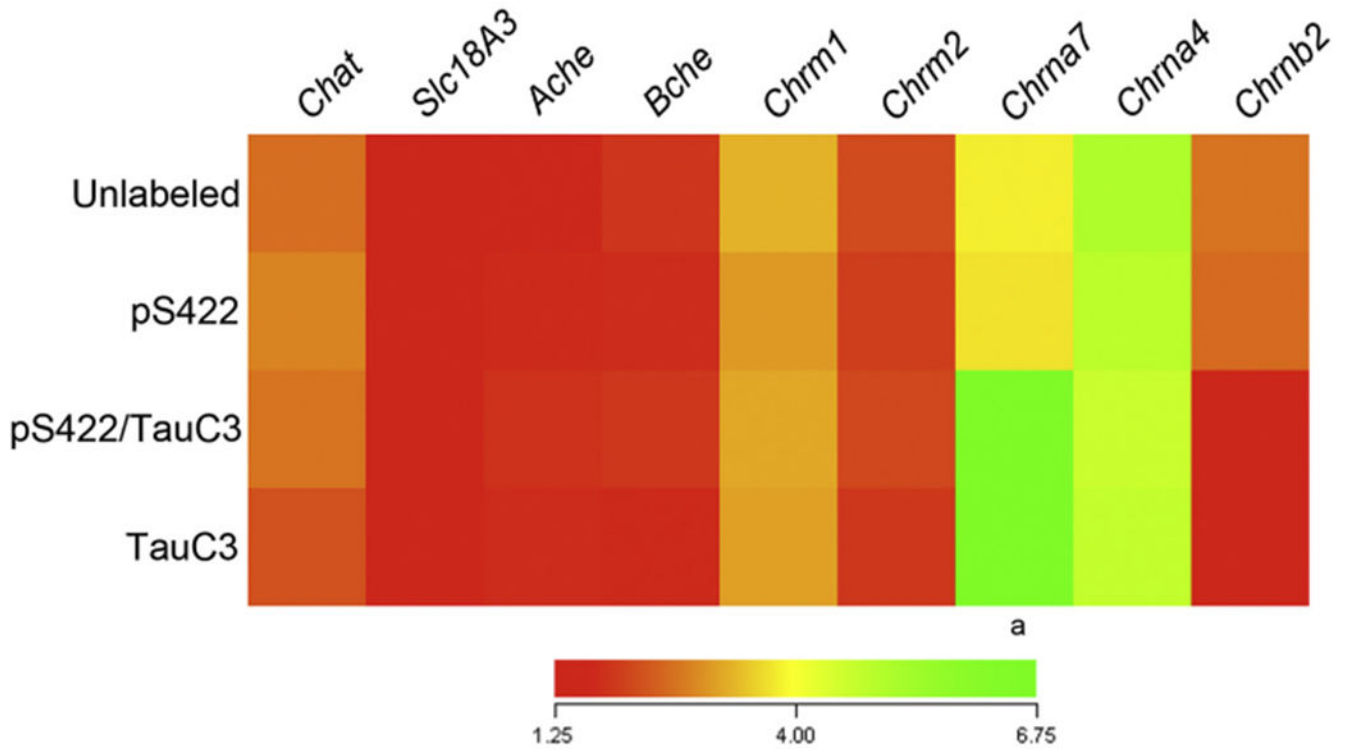


Fig. 4. Select cholinergic markers are dysregulated during the development of NFTs in nbM neurons. Heatmap of relative expression levels of cholinergic neuronal markers in pS422+, pS422+/TauC3+, and TauC3+ NB neurons compared to unlabeled control neurons (red to green = increasing mRNA levels). Quantitative analysis revealed upregulation of the *Chrna7* transcript and downregulation of the *Chrb2* transcript following the appearance of the TauC3 epitope. Abbreviations: *Chat* choline acetyltransferase; *Slc18a3*, vesicular acetylcholine transporter; *Ache*, acetylcholinesterase; *Bche*, butyrylcholinesterase; *Chrm1*, *Chrm2*, cholinergic receptor, muscarinic 1, 2; *Chrna7*, *Chrna4*, *Chrb2*, cholinergic receptor, nicotinic, alpha polypeptide 7, alpha polypeptide 4, beta polypeptide 2. a, pS422 < pS422+/TauC3+, $p < 0.01$; b, pS422 > pS422+/TauC3+, $p < 0.05$.

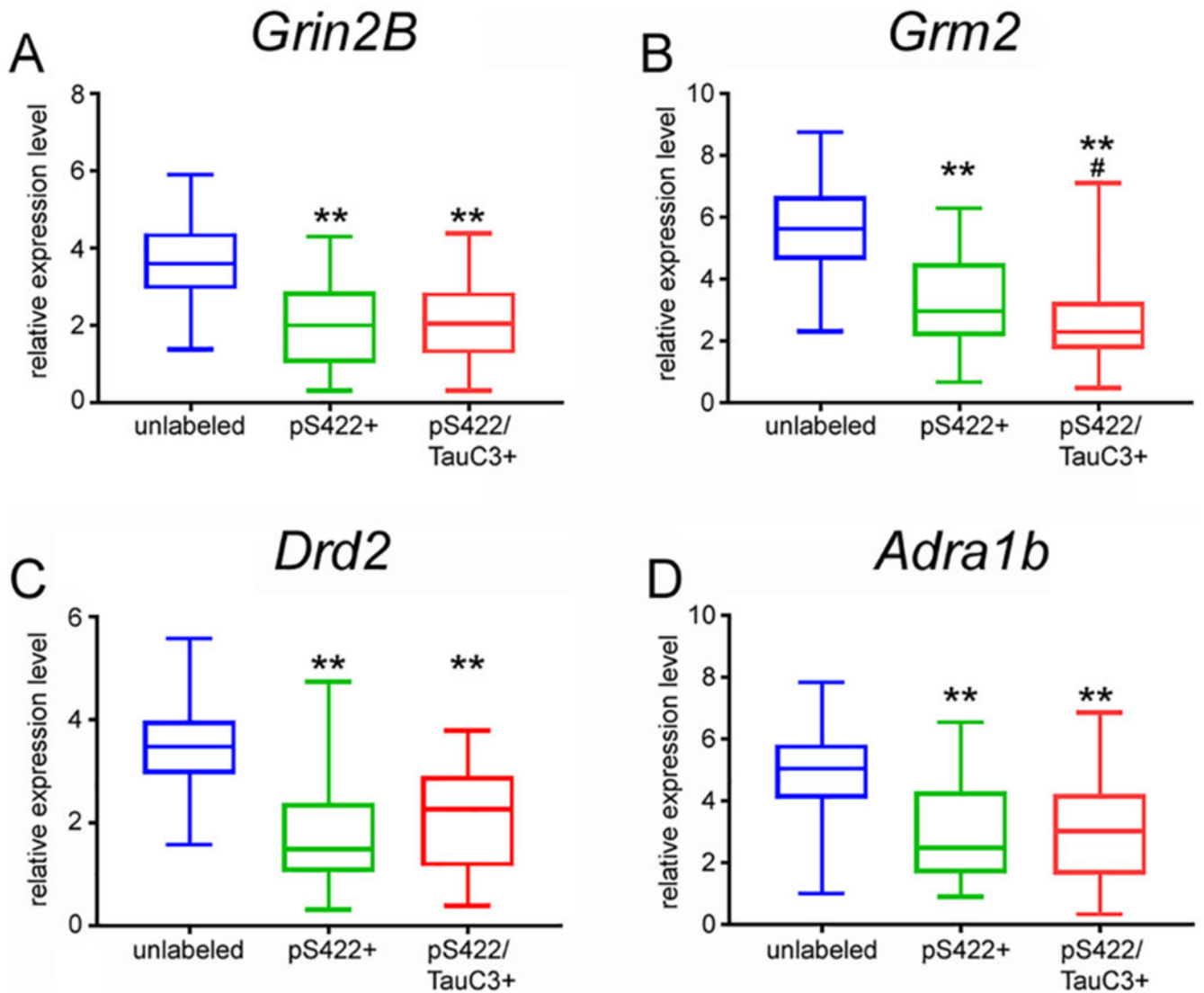


Fig. 5. Downregulation of select glutamatergic, dopaminergic, and noradrenergic receptors in pretangle-bearing nbM neurons. Boxplots show significant down-regulation in (A) the *Grin2B* NMDA receptor subunit, (B) *Grm2* metabotropic glutamate receptor 2, (C) *Drd2* D2 dopamine receptor, and (D) *Adra1b* β 1 adrenoceptor in pS422+ neurons compared to unlabeled neurons. This downregulation persisted pS422+/TauC3+ neurons. Expression levels of these transcripts were similar between pS422+/TauC3+ and TauC3+ neurons. ** $p < 0.001$, #, $p < 0.05$, pS422+ > pS422+/TauC3+.

Table 1

Clinical, demographic, and neuropathological characteristics by diagnosis category.

	Clinical diagnosis			AD (N = 8)	p-Value	Pair-wise comparison
	NCI (N = 10)	aMCI (N = 10)	AD (N = 8)			
Age (years) at death	Mean ± SD (Range) 84.6 ± 4.3 (78–92)	85.4 ± 3.9 (79–91)	84.7 ± 5.0 (76–88)	0.6 ^a	-	
Number (%) of males	5 (50%)	5 (50%)	3 (38%)	0.5 ^b	-	
Years of education	Mean ± SD (Range) 18.7 ± 1.6 (16–21)	17.5 ± 4.3 (15–25)	19.1 ± 3.5 (16–24)	0.2 ^a	-	
Number (%) with ApoE ε4 allele	1 (10%)	3 (33%)	4 (50%)	0.007 ^b	NCI < AD	
MMSE	Mean ± SD (Range) 27.8 ± 1.6 (26–30)	27.4 ± 2.7 (22–30)	22.1 ± 5.3 (15–26)	<0.001 ^a	(NCI, MCI) > AD	
Global Cognitive Score	Mean ± SD (Range) 0.04 ± 0.3 (-0.4–0.4)	-0.06 ± 0.3 (-1.2 to -0.2)	-1.3 ± 0.4 (-2.0 to -0.9)	<0.0001 ^a	NCI > MCI > AD	
Post-mortem interval (h)	Mean ± SD (Range) 5.9 ± 2.5 (3.3–9.0)	6.0 ± 2.6 (2.0–10.0)	5.5 ± 4.0 (2.5–12.0)	0.5 ^a	-	
Distribution of Braak scores	0	0	0	0.004 ^a	NCI < (MCI, AD)	
NIA Reagan diagnosis (likelihood of AD)	No AD	0	0	0.002 ^a	NCI < (MCI, AD)	
	Low	6	3			
	Intermediate	3	5			
	High	1	2			
CERAD diagnosis	No AD	3	0	0.01 ^a	(NCI, MCI) < AD	
	Possible	4	3			
	Probable	3	3			
	Definite	0	1			

^aKruskal-Wallis test, with Bonferroni correction for multiple comparisons.

^bFisher's exact test, with Bonferroni correction for multiple comparisons.

Table 2

Diagnostic group differences for select neurotransmitter receptor genes within nbM neurons with varying tau pathology.

Transcript	<i>p</i> -Value	Groupwise comparison
<i>Gria1</i>	0.002	pS422/TauC3 < unlabeled, pS422
<i>Gria2</i>	0.001	pS422/TauC3 < unlabeled, pS422
<i>Gria3</i>	n.s.	
<i>Gria4</i>	n.s.	
<i>Grik1</i>	0.02	pS422/TauC3 < unlabeled, pS422
<i>Grik2</i>	n.s.	
<i>Grik3</i>	n.s.	
<i>Grik4</i>	0.04	pS422/TauC3 < unlabeled, pS422
<i>Grik5</i>	n.s.	
<i>Grin1</i>	0.005	pS422/TauC3 < unlabeled, pS422
<i>Grin2a</i>	n.s.	
<i>Grin2b</i>	0.001	pS422, pS422/TauC3 < unlabeled
<i>Grin2c</i>	n.s.	
<i>Grin2d</i>	n.s.	
<i>Grm1</i>	n.s.	
<i>Grm2</i>	< 0.001	pS422/TauC3 < pS422 < unlabeled
<i>Grm3</i>	n.s.	
<i>Grm4</i>	n.s.	
<i>Grm5</i>	n.s.	
<i>Grm6</i>	n.s.	
<i>Grm7</i>	n.s.	
<i>Grm8</i>	n.s.	
<i>Gabra1</i>	n.s.	
<i>Gabra2</i>	n.s.	
<i>Gabra3</i>	n.s.	
<i>Gabra4</i>	n.s.	
<i>Gabra5</i>	n.s.	
<i>Gabra6</i>	n.s.	
<i>Gabrb1</i>	n.s.	
<i>Gabrb2</i>	0.04	pS422/TauC3 < unlabeled, pS422
<i>Gabrb3</i>	n.s.	
<i>Gabrd</i>	n.s.	
<i>Gabbr1</i>	0.05	pS422/TauC3 < unlabeled, pS422
<i>Drd1</i>	0.02	pS422/TauC3 < unlabeled, pS422
<i>Drd2</i>	< 0.001	pS422, pS422/TauC3 < unlabeled
<i>Drd3</i>	n.s.	
<i>Drd4</i>	0.008	pS422/TauC3 < unlabeled, pS422
<i>Drd5</i>	n.s.	

Transcript	<i>p</i> -Value	Groupwise comparison
<i>Adra1b</i>	< 0.001	pS422, pS422/TauC3 < unlabeled
<i>Adra2a</i>	0.003	pS422/TauC3 < unlabeled, pS422
<i>Adra2b</i>	0.005	pS422/TauC3 < unlabeled, pS422
<i>Htr1b</i>	n.s.	
<i>Htr2b</i>	0.03	pS422/TauC3 < unlabeled, pS422
<i>Htr2c</i>	n.s.	
<i>Htr3</i>	n.s.	
<i>Htr7</i>	n.s.	
<i>Galr1</i>	n.s.	
<i>Galr2</i>	n.s.	
<i>Galr3</i>	n.s.	

n.s.: not significant.

See Abbreviations.

Author Manuscript

Author Manuscript

Author Manuscript

Author Manuscript

Linear regression analysis for association between clinical pathologic status and expression levels of select receptor genes within unlabeled and pS422+ nbM neurons.

Table 3

Gene ID	Cell phenotype	GCS	MMSE	Braak	CERAD	Reagan
<i>Nr1k1</i> TK	Unlabeled	p = 0.01	p = 0.09	p = 0.04	p = 0.2	p = 0.1
	pS422+	p = 0.007	p = 0.05	p = 0.02	p = 0.1	p = 0.04
<i>Nr1k2</i> TK	Unlabeled	p = 0.01	p = 0.1	p = 0.03	p = 0.1	p = 0.1
	pS422+	p = 0.008	p = 0.06	p = 0.01	p = 0.3	p = 0.08
<i>Nr1k3</i> TK	Unlabeled	p = 0.2	p = 0.6	p = 0.3	p = 0.3	p = 0.6
	pS422+	p = 0.01	p = 0.2	p = 0.08	p = 0.5	p = 0.4
<i>Gria2</i>	Unlabeled	p = 0.4	p = 0.5	p = 0.3	p = 0.8	p = 0.5
	pS422+	p = 0.06	p = 0.1	p = 0.05	p = 0.3	p = 0.1
<i>Grin2b</i>	Unlabeled	p = 0.03	p = 0.1	p = 0.05	p = 0.09	p = 0.1
	pS422+	p = 0.006	p = 0.05	p = 0.01	p = 0.2	p = 0.06
<i>Gria2</i>	Unlabeled	p = 0.2	p = 0.4	p = 0.08	p = 0.7	p = 0.5
	pS422+	p = 0.05	p = 0.1	p = 0.1	p = 0.5	p = 0.2
<i>Drd2</i>	Unlabeled	p = 0.07	p = 0.1	p = 0.1	p = 0.6	p = 0.5
	pS422+	p = 0.01	p = 0.07	p = 0.09	p = 0.2	p = 0.2
<i>Adrab1</i>	Unlabeled	p = 0.05	p = 0.1	p = 0.06	p = 0.3	p = 0.1
	pS422+	p = 0.008	p = 0.06	p = 0.02	p = 0.09	p = 0.05

Boldface: significant association.